AERODYNAMICS OF A RECTANGULAR WING WITH A PERIPHERAL JET FOR AIR CUSHION TAKE-OFF AND LANDING

K. DAU, B. ETKIN and D. SURRY

UNIVERSITY OF TORONTO

FOREWORD

This report was prepared by the Institute for Aerospace Studies, University of Toronto, Ont., Canada. Financial support for the work was received from the Defence Research Board of Canada, the U.S.A.F. Research and Technology Division, Flight Dynamics Laboratory, Control Criteria Branch (Contract AF-33(657) 8451) and the Vertol Division, Boeing Aircraft Co. The investigation was conducted from May 1959, to Sept. 1964 The contract was initiated under Project No. 8219 "Stability and Control Investigations", Task No. 821907, "V/STOL Aerodynamic Stability and Control". Contributions to this study were provided by Messrs. K. Dau, J. M. Davis, and D. Surry, who carried out the experimental work and the data analysis. Professor B. Etkin served as principal investigator and supervisor.

Manuscript released by authors May 31, 1965, for publication as an RTD Technical Report.

This Technical Report has been reviewed and is approved.

C.B. Westbrook

C. B. WESTBROOK
Chief, Control Criteria Branch
Flight Control Division

ABSTRACT

Subsonic wind tunnel experiments on a GETOL wing are reported. The main results relevant to performance, stability and control are presented, and applied to a hypothetical vehicle. Short-field capability is demonstrated to be possible. Stability and control problems are analysed, and shown not to be prohibitive.

TABLE OF CONTENTS

ILLUSTRATIONS

TABLES

SYMBOLS

a	forward acceleration of aircraft, ft/sec^2
a_t	rate of change of C_{L_t} with respect to α, $deg.^{-1}$
A_j	jet slot area, ft^2
AR	wing aspect ratio
c	chord length, ft.
C_M	pitching moment coefficient, M/qSc
C_{M_α}	$\frac{\partial C_M}{\partial \alpha}$, $deg.^{-1}$
C_L	lift coefficient, L/qS
C_{L_t}	tail lift coefficient, L_t/qS
C_{L_α}	$\frac{\partial C_L}{\partial \alpha}$, $deg.^{-1}$
C_μ	J/qS
D	drag of wing due only to forward speed and air cushion, lb.
D_{mom}	drag due to engine inlet momentum, lb.
g	gravitational acceleration, $32.2\ ft/sec^2$
h'	height above ground, ft, measured from jet exit plane
H	drop height defined by Eq. 21, ft.
j	momentum flux per unit slot length $\int_0^{z_s} \rho V_j^2 dz$, lb/ft
J	total momentum flux of the peripheral jet $\int_{A_j} \rho V_j^2 dA_j$, lb.
J_1	jet momentum flux from leading edge slot, lb.
J_2	jet momentum flux from trailing edge slot, lb.

SYMBOLS (continued)

J_3	jet momentum flux from tip slots, lb.
J_D	momentum flux used for direct thrust, lb., = T_D
J_T	total installed thrust, lb., = $J + J_D$
l_t	length of tail, defined in Fig. 16, ft.
L	total lift on aircraft, lb.
L_t	lift on tail, lb.
L_w	lift on wing, lb.
m	mass of aircraft, slugs
M	pitching moment of aircraft about C.G., lb-ft.
M_w	pitching moment of wing about C.G., lb-ft.
$(M_w)_{c/2}$	pitching moment of wing about half-chord point, lb-ft.
p_i	static pressure at air inlet of model wing, lb/ft^2
q	dynamic pressure due to forward speed, $\frac{1}{2} \rho V^2$, lb/ft^2
q_{ic}	dynamic pressure at center of air inlet of model wing, lb/ft^2
$\bar{q}_j$	average jet dynamic pressure at slot exit, $J/2A_j$, lb/ft^2
R_1	ground run distance from hovering to transition, ft.
R_2	distance covered during transition at take-off, ft.
R_3	distance covered during steady climb over 50 ft. obstacle, ft.
R_4	ground run distance for landing, ft.
S	wing area, ft^2
S_t	area of horizontal tail, ft^2

SYMBOLS (continued)

T	thrust on wing due to forward speed and air cushion, lb.
T_D	direct engine thrust
T_r	recovered thrust defined by Eq. 2, lb.
V	forward speed of aircraft, ft/sec.
V_j	velocity of jet at slot exit, ft/sec.
V_z	vertical speed of aircraft, ft/sec.
V_H	horizontal tail volume, $\frac{S_t \ell_t}{S c}$
w	wing loading, lb/ft.
W	overall weight of aircraft, lb.
x	non-dimensional position of C.G., as defined in Fig. 16
x_n	non-dimensional position of neutral point
x_w	non-dimensional position of center of pressure of wing as defined in Fig. 16
α	geometrical angle of attack
ρ	mass density of air, slugs/ft^3
θ_1	angle of leading edge jet } measured from the vertical, positive for rearward deflection
θ_2	angle of trailing edge jet } measured from the vertical, positive for rearward deflection
τ	distance across slot, ft.
τ_s	slot width, ft.
γ	angle of climb

Section 1

INTRODUCTION

The idea of replacing a normal airplane undercarriage with the air cushion trapped between a peripheral-jet wing and the ground was suggested explicitly as early as 1957 by Von Glahn[1] and was a consideration even earlier at Avro Aircraft, Canada, during the developments that preceded the AVROCAR [2]. In the intervening years several studies of the potentialities of this concept (GETOL) have been carried out (Refs. 3 to 9). The Vertol [4] and Convair [5] studies of subsonic airplanes both indicated some potential from a performance standpoint for this class of aircraft when compared with VTOL airplanes to perform the same mission. Alexander's [6] work indicated that the application of a peripheral jet to a low aspect ratio delta wing would enable take-off and landing distances of a large supersonic transport airplane to be reduced to about 1/2 the normal value.

An experimental study of a GETOL wing was also started at UTIAS in 1959. Detailed measurements were undertaken of the aerodynamic characteristics relevant to performance and stability of a rectangular wing of aspect ratio 4, with a peripheral jet encompassing the entire perimeter, when in close proximity to the ground. This wing shape was expected to provide a reasonable compromise between the air cushion and cruise requirements. The results of the tests have been reported in References 7, 8 and 9. Further research is currently under way utilizing a second half-wing model with a rounded tip and improved internal and external flow characteristics.

The aim of this investigation was primarily to assess the problems of take-off and landing of a GETOL aircraft and to determine whether or not it has the basic capability to compete with other forms of STOL aircraft. The crucial question is whether it can take off in short-field distances, i.e., less than 1500 ft., to clear a 50-ft. obstacle, with installed thrust to weight ratios significantly less than one.

The GETOL concept has, of course, a great appeal by virtue of the ability of this kind of airplane to take off and land on relatively unprepared surfaces. Turf, water or snow are all possible landing surfaces. The only requirement is that it needs to be approximately level. For example, a golf course fairway could provide a suitable landing strip. The advantage in operational flexibility achieved, when combined with the weight saved by doing away with the undercarriage, may offer the necessary economic

advantages to offset the penalties which such a configuration would necessarily impose (i. e., provision of jet curtain, internal ducting, hovering stability and control problems, loss of cruise performance). An assessment of the overall design problem is not the purpose of this report. It is concerned entirely with the aerodynamic properties of the wing as they relate to the performance and stability aspects of take-off and landing. The application of this information to design studies is more properly the work of industry. Thus in the following we present the main results of the tests reported in Refs. 7, 8 and 9, and their application to calculations of take-off and landing distance, and to the problems of trim and stability.

Section 2

EXPERIMENTAL INVESTIGATION

2.1 Outline of Experiments

The lift, drag and pitching moment on a model wing with a peripheral jet (see Figs. 1 and 2) were measured in the UTIAS subsonic wind tunnel for a range of angles of attack, forward speeds, heights above ground, and jet angles. Considerable effort was expended in measuring the distribution of j along the peripheral slot (see Fig. 3). Flow visualisation tests utilising lampblack and kerosene on the ground board were also made (see Fig. 4). A list of all the configurations tested appears in Table 1. For a complete description of the wing model and the experimental investigation see Refs. 7, 8 and 9.

2.2 Experimental Results

The results of the force and moment measurements are presented in Ref. 7, 8 and 9 in the form of non-dimensional graphs. A representative sample of the results from Ref. 8, replotted in a different coordinate system, is given in Figs. 5 to 9, for the 0^o -jet configuration shown in the inset on Fig. 5. Figures 5 to 8 give the lift, drag, and pitching moment data for a range of α and forward speeds, at a fixed height, $h'/c = .108$; and Fig. 9 gives the center of pressure for the same conditions. Another set of results (from Ref. 9) is given in Figs. 10 and 11. These are for a variety of configurations, all at $\alpha = 0$ and $h'/c = 0.108$, and present the lift and thrust/drag data needed for take-off and landing calculations. The particular configurations tested were chosen in an attempt to maximize the acceleration at each speed during the take-off run.

The data show that at low forward speeds the wing with peripheral jet behaves essentially like a hovering air-cushion vehicle, whereas at high speeds it exhibits jet-flap characteristics, (linear variation of C_L with $\sqrt{C_\mu}$, see Fig. 12). The transition from the air-cushion regime to the jet-flap regime is gradual rather than abrupt, as exemplified by the smooth variation of the force coefficients with forward speed shown in Figs. 5 to 8. The explanation for the smooth transition is found in the behavior of the leading edge jet with increasing forward speed. At low forward speeds only a small portion in the center of the leading edge jet is deflected back underneath the wing. As the forward speed increases, this portion grows gradually until all of the leading edge jet is eventually blown back under the wing. This process

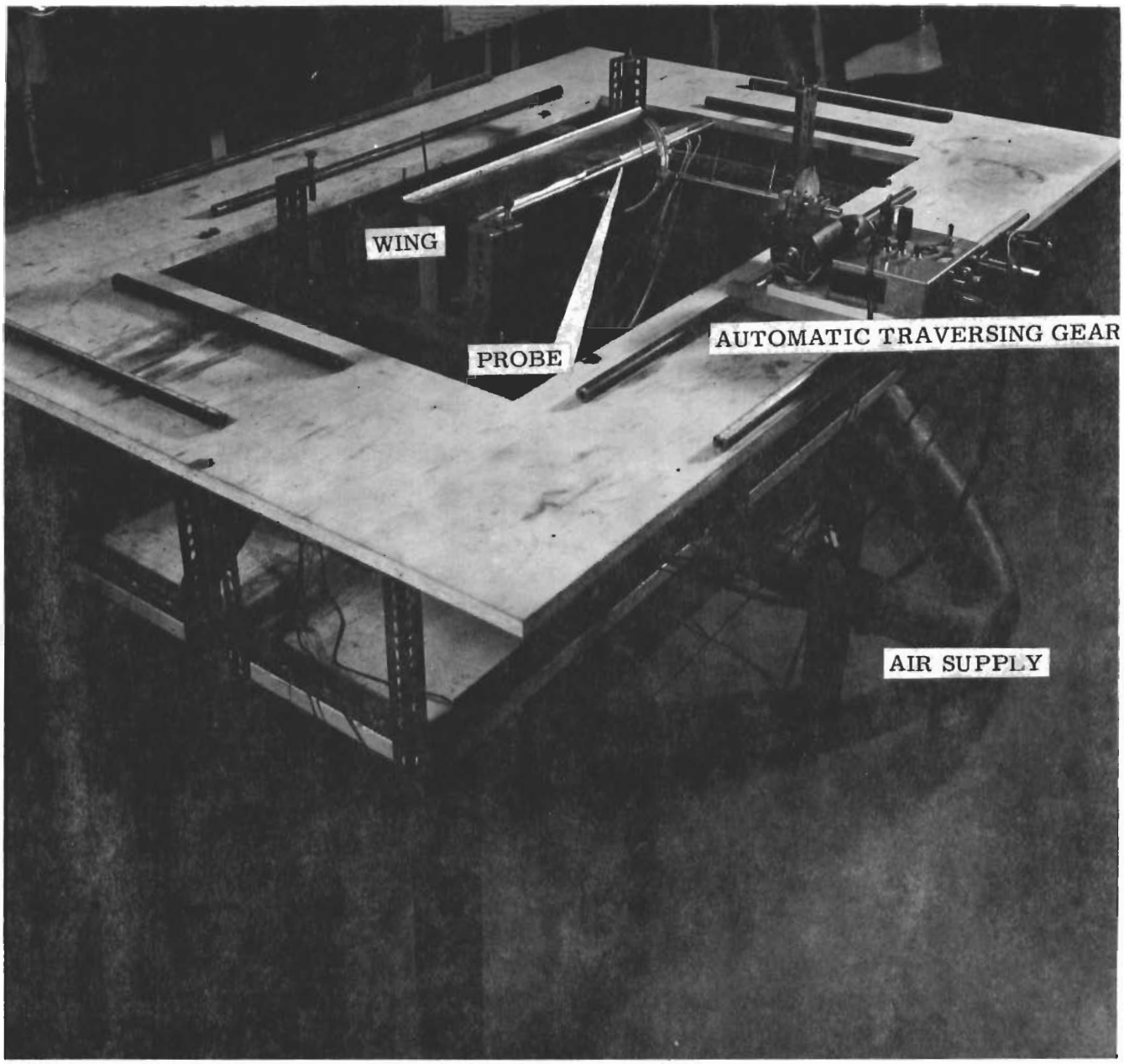

FIG. 1 WING MOUNTED IN CALIBRATION RIG

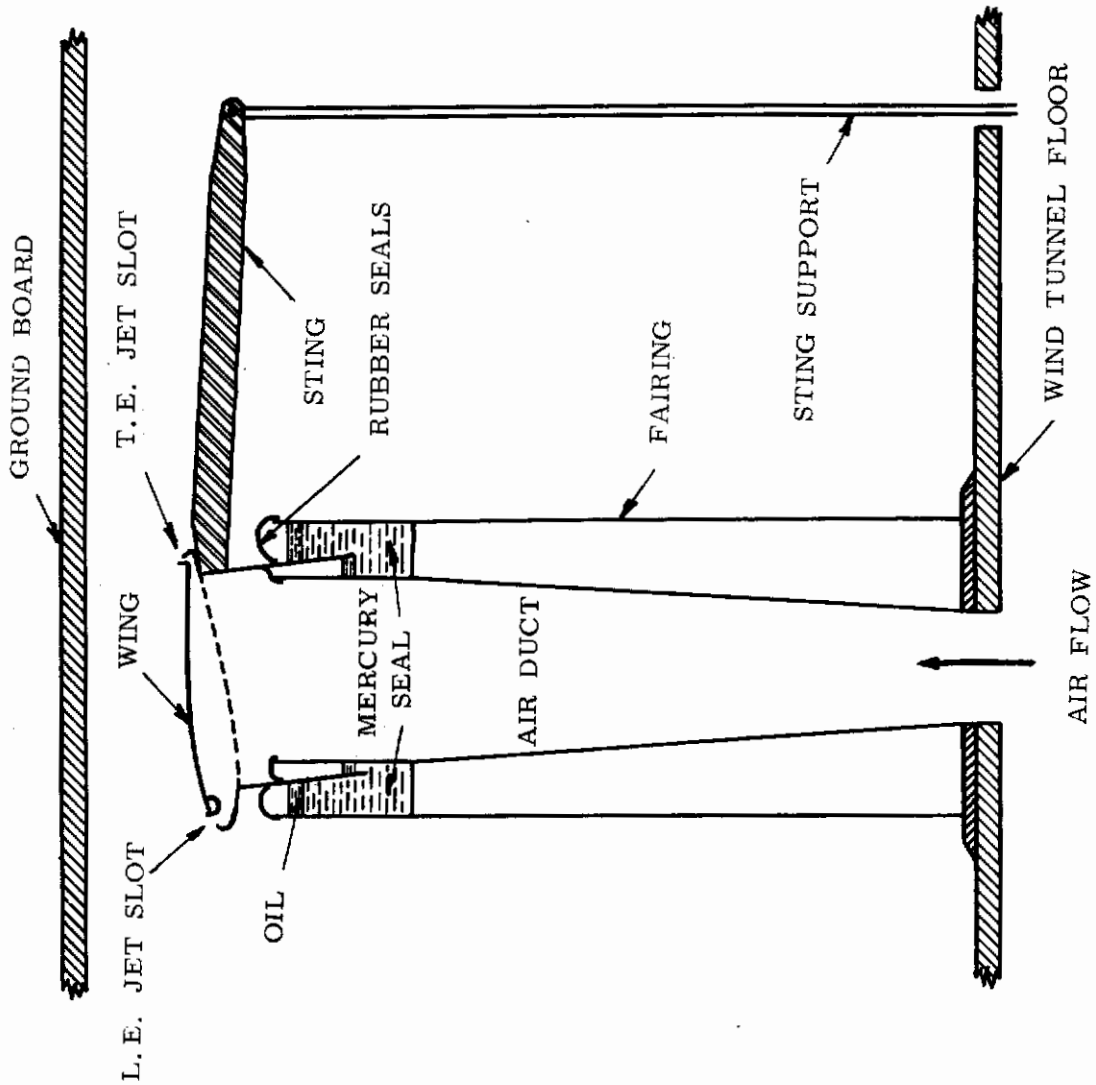

FIG. 2 SCHEMATIC CROSS-SECTION OF BLOWING WING AS INSTALLED IN UTIAS SUBSONIC WIND TUNNEL

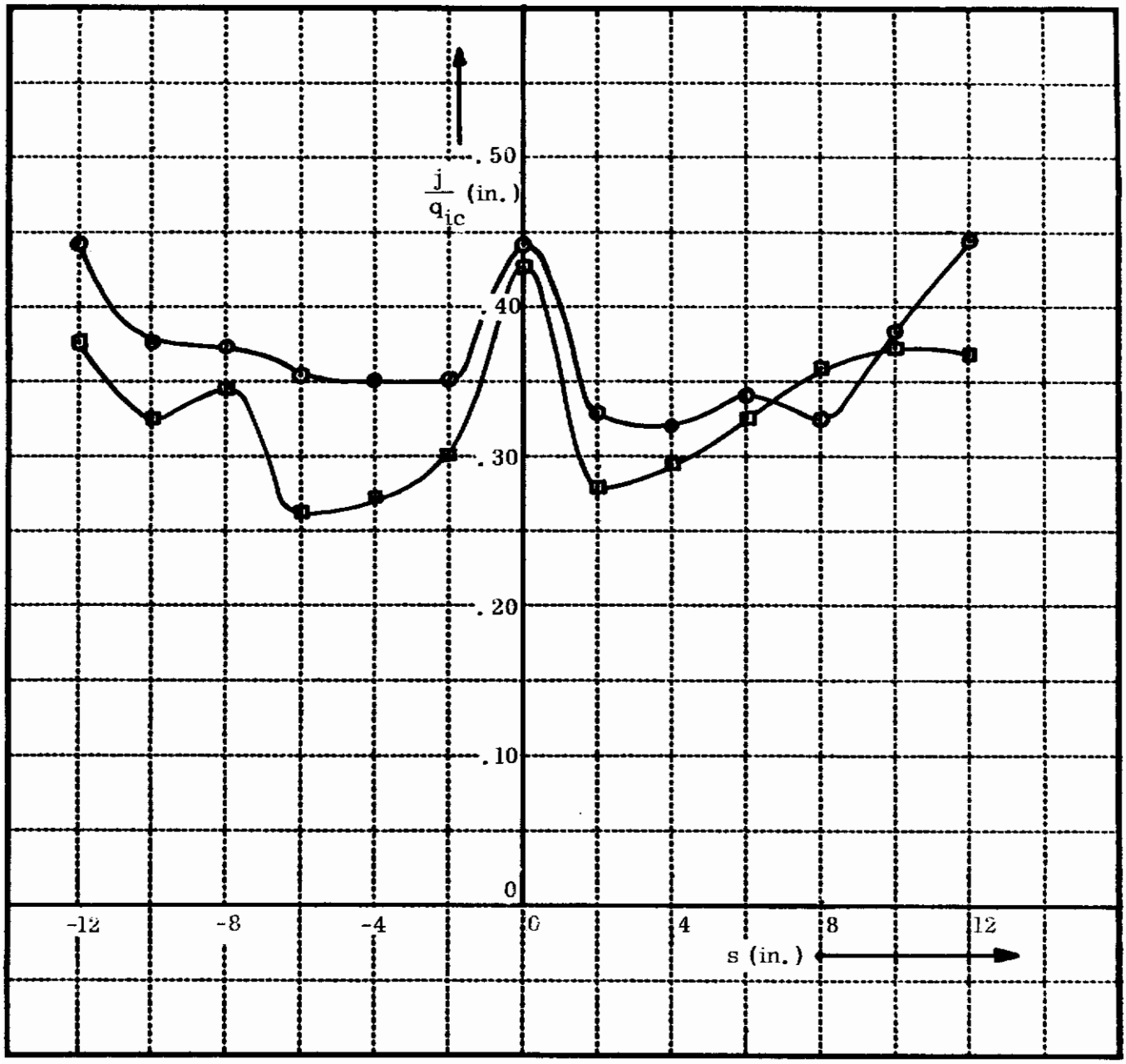

FIG. 3 LOCAL JET MOMENTUM FLUX PER UNIT SLOT LENGTH IN THE STREAMWISE PLANE (Ref. 8)

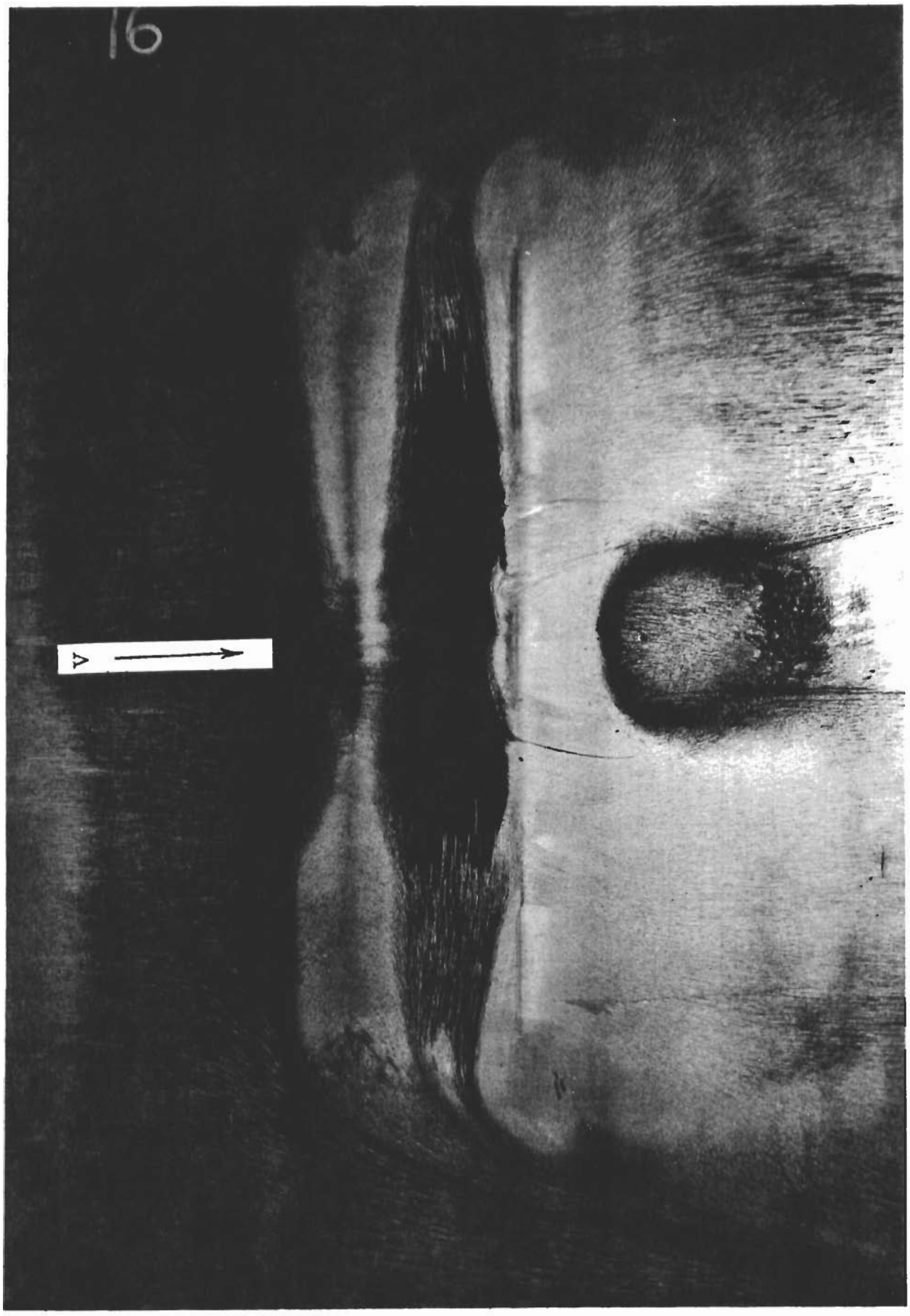

FIG. 4 GROUND STREAK PATTERN C10

$\frac{h'}{c} = 0.1, \quad \alpha = 7.5, \quad \frac{qS}{J} = 4.0$

CONFIG.	J_1/J	J_2/J	J_3/J	J_1/J_2	Θ_1	Θ_2	Θ_2/Θ_1	$\frac{2A_i}{S} \times 10^2$
1	o. 435	o. 340	o. 225	1. 28	22. 8	-29. 4	-1. 29	8. 67
2	o. 397	o. 355	o. 249	1. 12	15. 0	-21. 5	-1. 43	9. 56
3	o. 478	o. 425	o. 097	1. 13	20. 0	- 2. 0	-o. 10	8. 91
4	o. 269	o. 566	o. 165	o. 475	21. 5	- o. 5	-o. 023	8. 85
5	o. 444	o. 446	o. 110	o. 997	23. 0	13. 5	o. 586	9. 61
6	o. 289	o. 580	o. 131	o. 498	21. 0	25. 0	1. 19	7. 61
7	o. 238	o. 661	o. 101	o. 360	25. 0	33. 0	1. 32	6. 96
8	o. 0	o. 870	0. 130	o. 0	-----	32. 5	-----	5. 76
9	o. 0	1. 00	o. 0	o. 0	-----	43. 5	-----	5. 83
10	o. 41	o. 41	o. 18	1. 00	o. 0	o. 0	-----	7. 26
11	o. 405	o. 405	o. 19	1. 00	30. 0	30. 0	1. 00	7. 02

TABLE 1 LIST OF CONFIGURATIONS TESTED

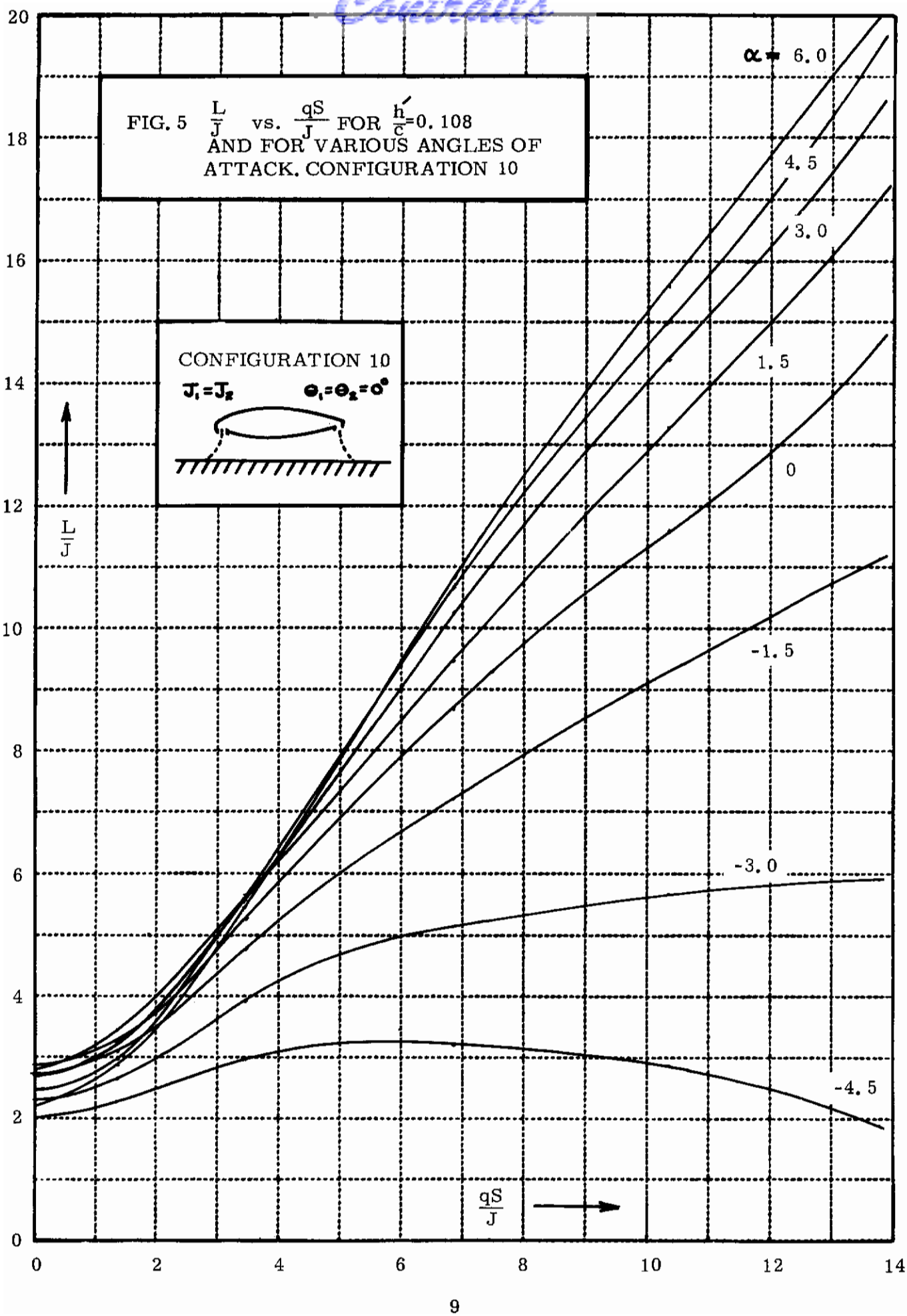

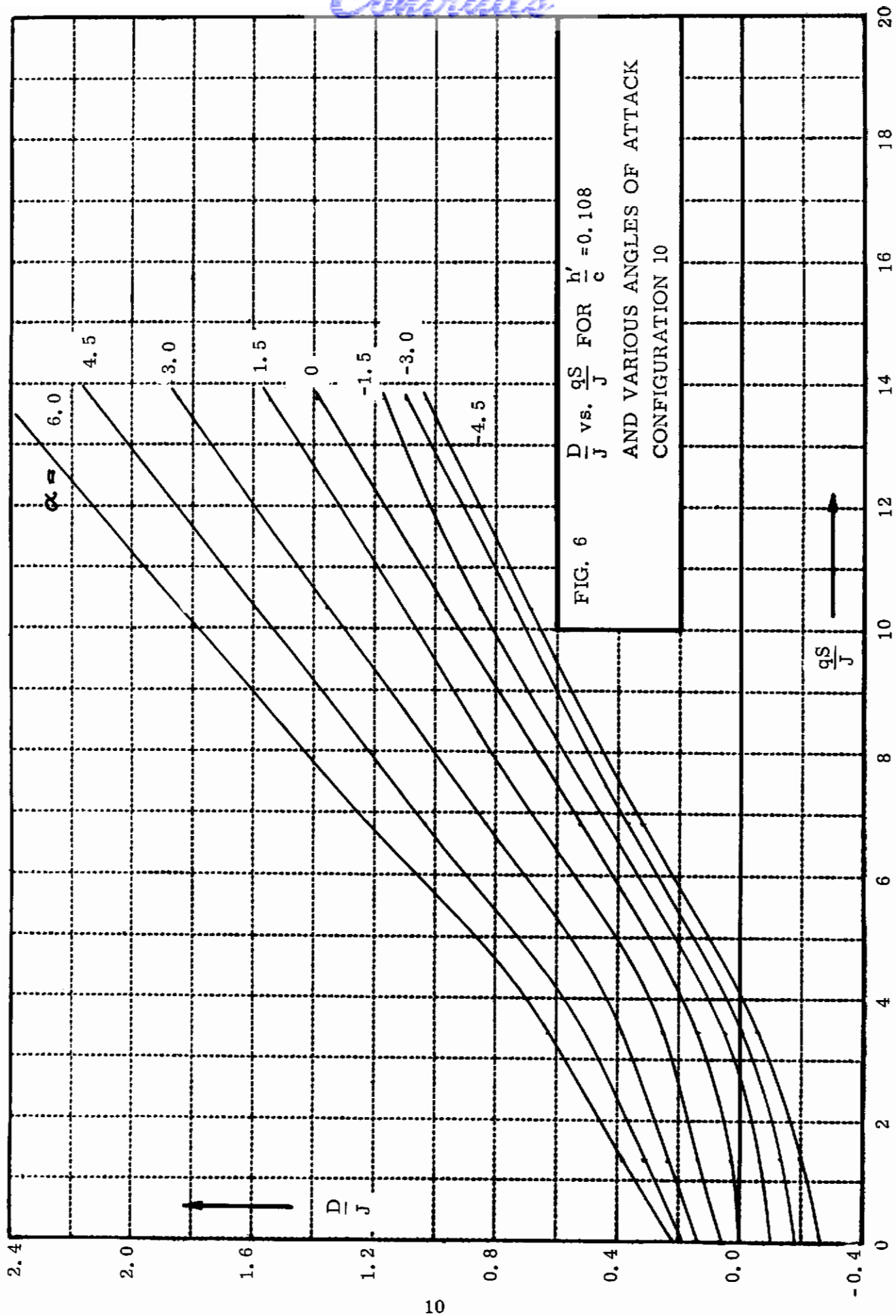

FIG. 6 $\frac{D}{J}$ vs. $\frac{qS}{J}$ FOR $\frac{h'}{c}$ =0.108 AND VARIOUS ANGLES OF ATTACK CONFIGURATION 10

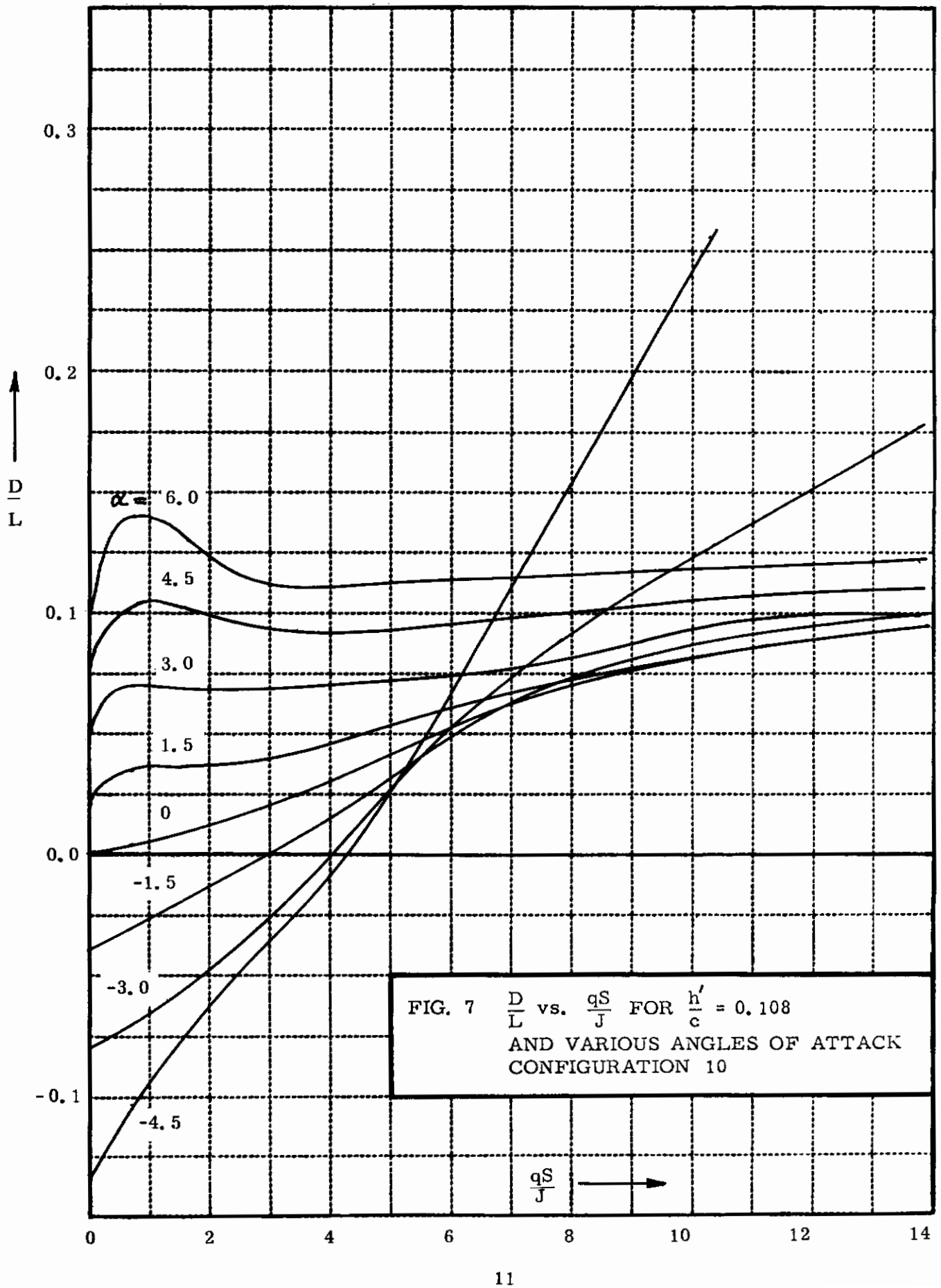

FIG. 7 $\frac{D}{L}$ vs. $\frac{qS}{J}$ FOR $\frac{h'}{c}$ = 0.108
AND VARIOUS ANGLES OF ATTACK
CONFIGURATION 10

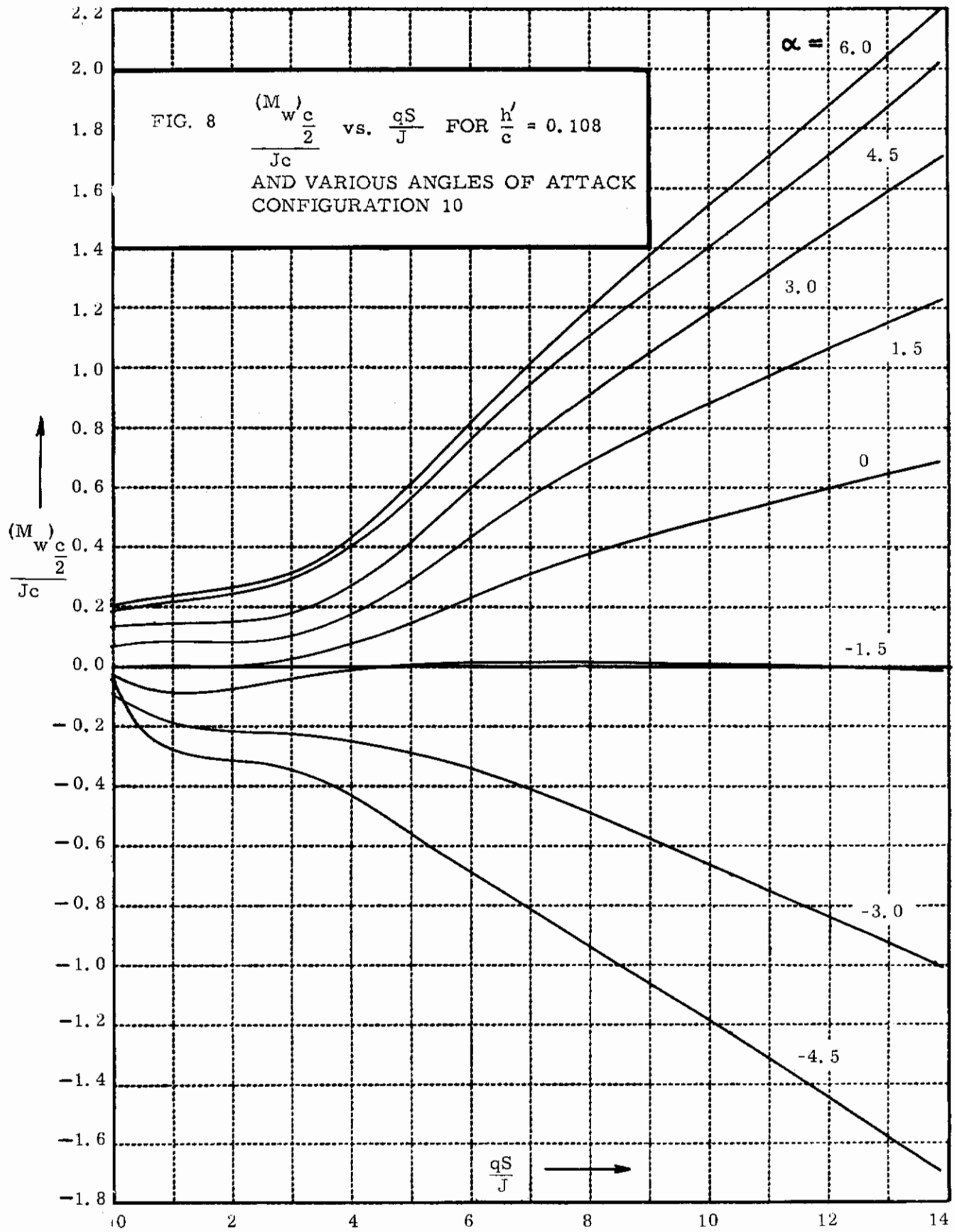

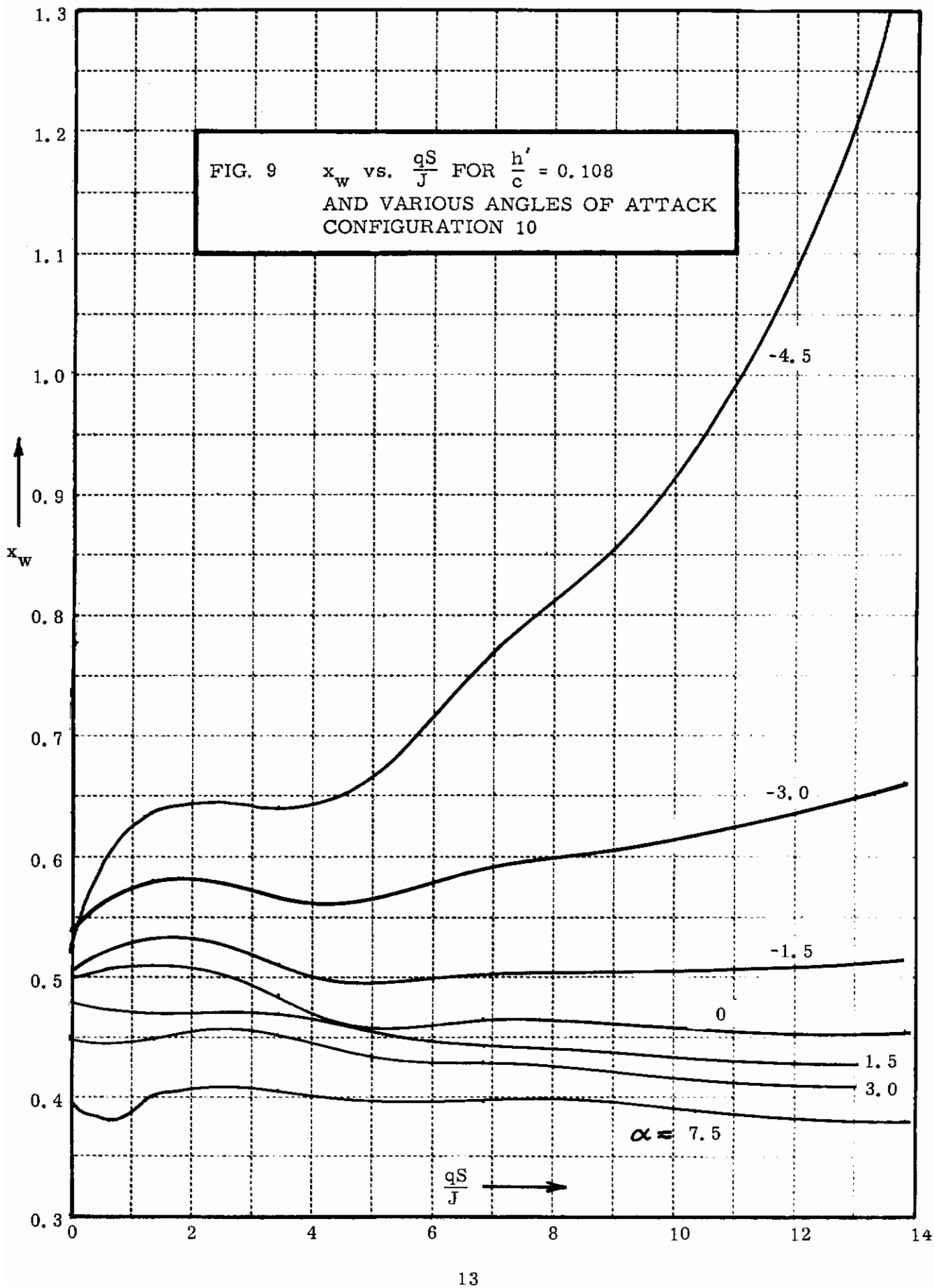

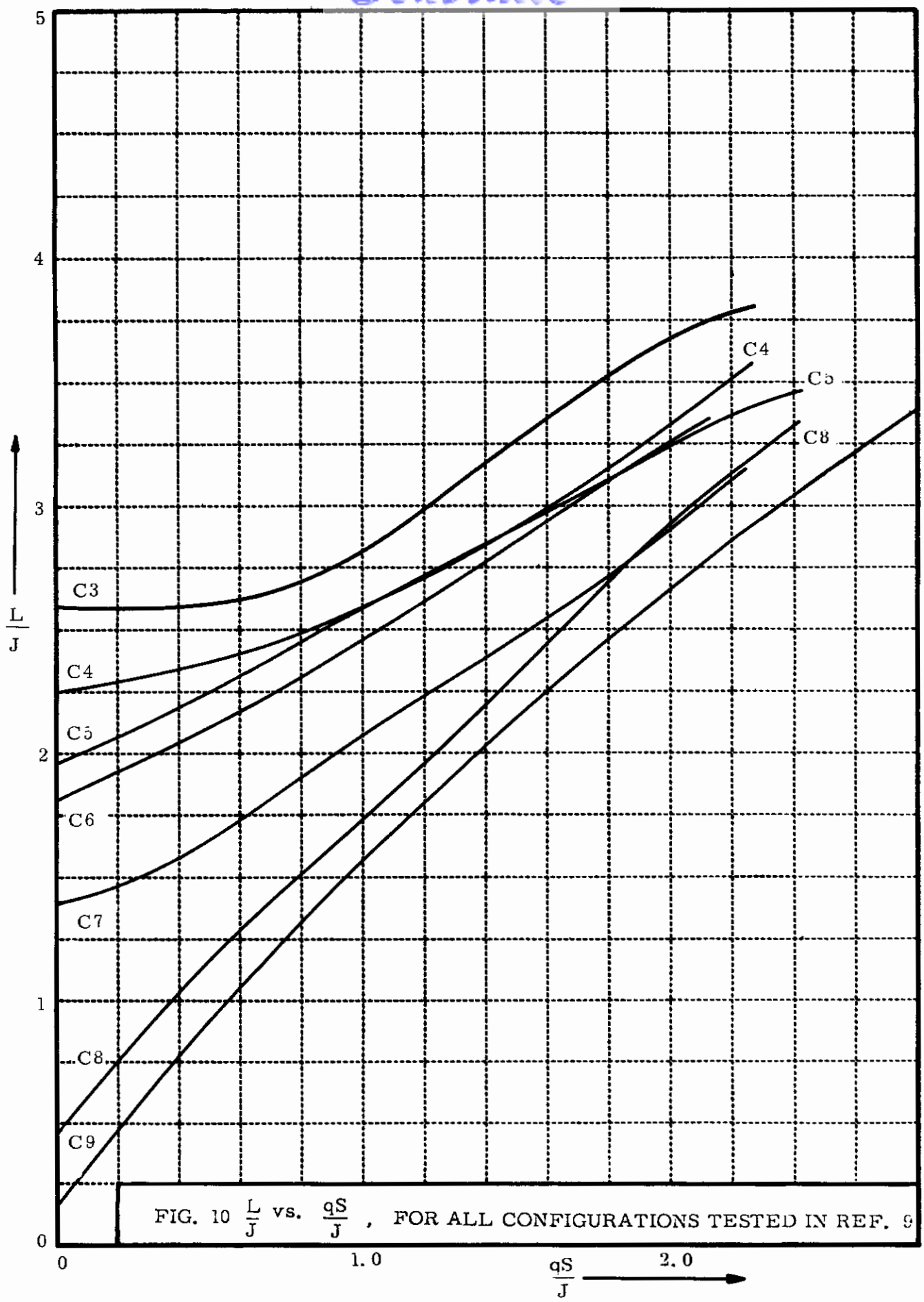

FIG. 10 $\frac{L}{J}$ vs. $\frac{qS}{J}$, FOR ALL CONFIGURATIONS TESTED IN REF. 9

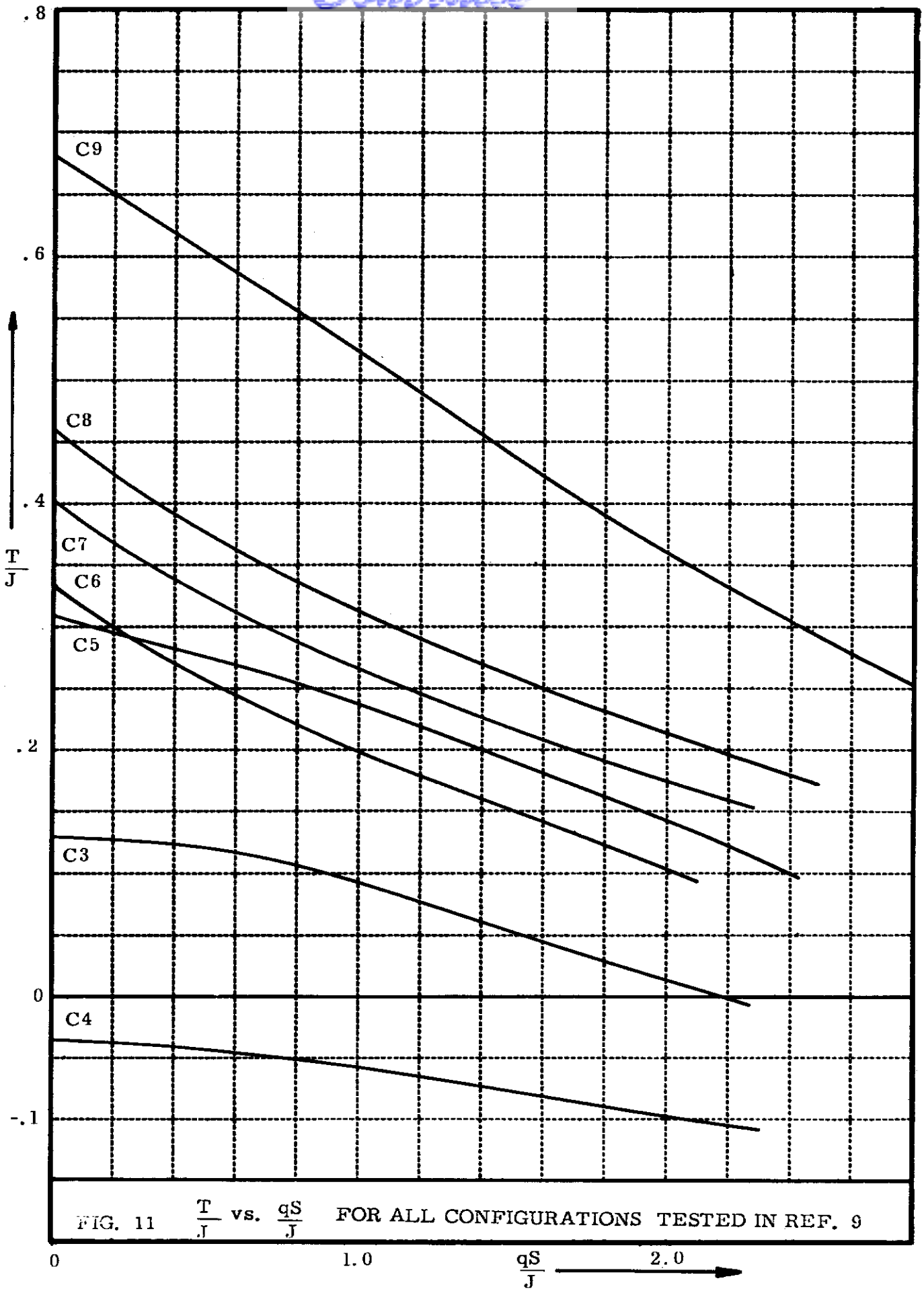

FIG. 11 $\frac{T}{J}$ vs. $\frac{qS}{J}$ FOR ALL CONFIGURATIONS TESTED IN REF. 9

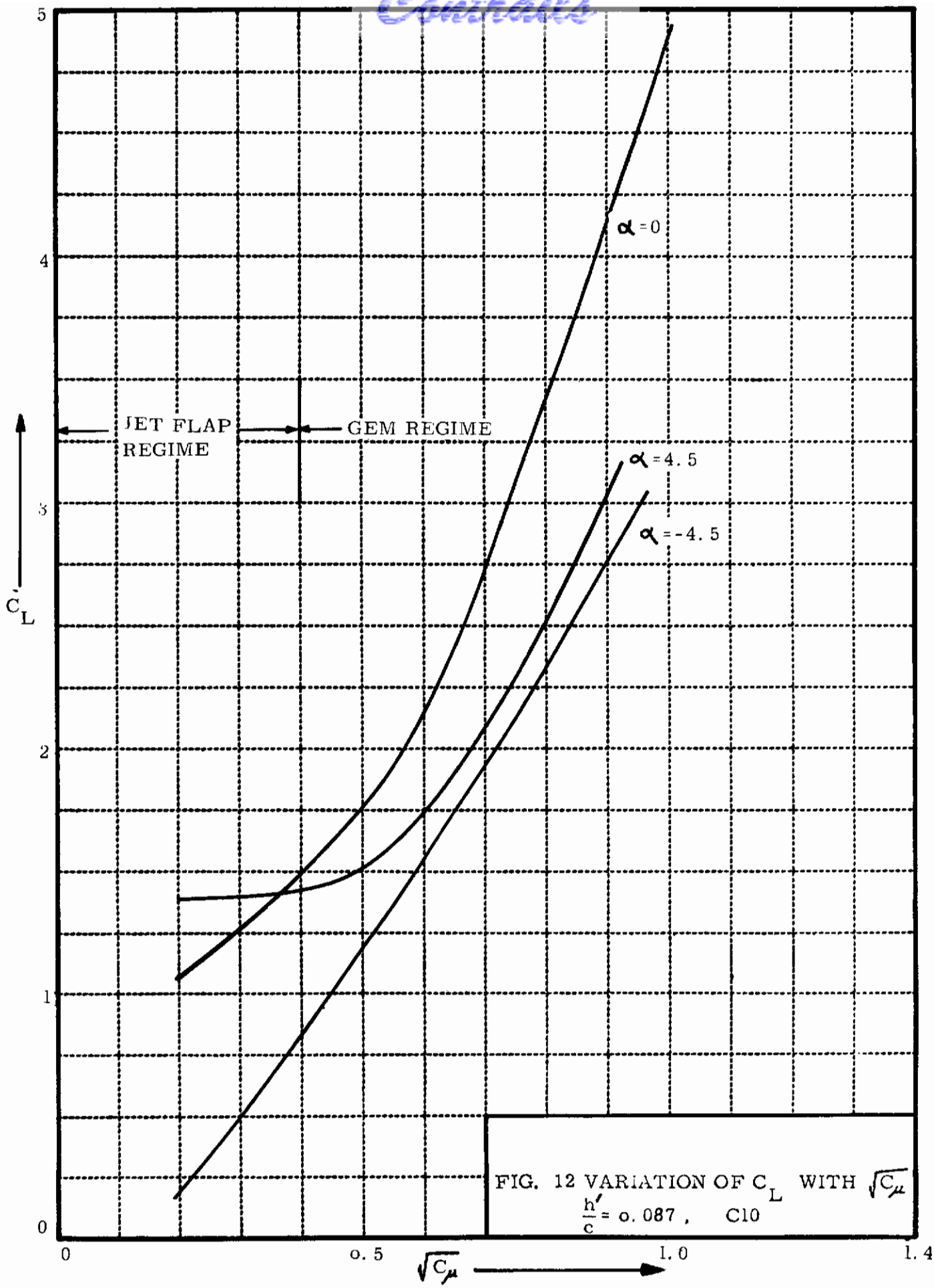

FIG. 12 VARIATION OF C_L WITH $\sqrt{C_\mu}$
$\frac{h'}{c} = 0.087$, C10

is completed over an appreciable forward-speed range (depending on height and angle of attack) and thus results in a fairly smooth transition from the air-cushion to the jet-flap regime.

As regards thrust recovery, the thrust hypothesis for jet-flapped wings predicts that all of the jet momentum flux from the wing is recovered as horizontal thrust owing to the bending of the jet sheet. A study of Fig. 7 indicates that some thrust recovery does occur, but only at low forward speeds and negative angles of attack. To determine the thrust being recovered the argument is used that the resultant force on the wing is perpendicular to the wing if zero thrust is recovered. In this case

$$T = -L \tan \alpha \quad \text{or} \quad D = L \tan \alpha \tag{1}$$

Hence any thrust larger than $-L \tan \alpha$ can be considered recovered thrust, T_r, i.e.

$$T_r = T - (-L \tan \alpha) \tag{2}$$

or

$$\frac{T_r}{J} = \frac{L}{J} \left(\frac{T}{L} + \tan \alpha\right)$$

$$= \frac{L}{J} \left(\tan \alpha - \frac{D}{L}\right)$$

From Fig. 7 one finds that D/L is smaller than $\tan \alpha$ only for negative angles of attack and low forward speeds. Hence thrust is recovered under these conditions only.

The pitching moment data showed typically that the wing alone is unstable, as exemplified by the positive slope of the $\frac{(M_w)_{c/2}}{Jc}$ vs α curve at $\frac{(M_w)_{c/2}}{Jc} = 0$ as can be inferred from Fig. 8. The corresponding neutral points lie generally in the range 0.25 to 0.50c depending on aerodynamic conditions, the lower value being associated with high forward speeds, and the larger value with hovering.

Section 3

APPLICATION TO TAKE-OFF

3.1 Description of Aircraft

In this section use is made of the experimental data to determine whether or not a GETOL aircraft has STOL capability. The hypothetical aircraft that is considered here has a wing, with a peripheral jet similar to the one under discussion, a conventional tail, engines for forward propulsion and engines that supply air to the peripheral slot. It may or may not have a mechanical arrangement by which some of the air from the lift engines can be diverted for forward propulsion. The combined installed thrust/weight ratio, J_T/W is fixed at 0.7, which is two-thirds of the thrust requirements for a VTOL aircraft. Following are the numerical values used throughout the analysis:

$W = 20,000$ lb.

$w = 20$ psf

$AR = 4.17$ (same as model wing)

$\left(\frac{J}{J_T}\right)_{max} = 0.5$

$\frac{J_T}{W} = 0.7$

$\frac{A_j}{S} = .0363$

This leads to

$h' = 1.67$ ft. for $h'/c = 0.108$

$J_T = 14,000$ lb.

$J_{max} = 7,000$ lb.

$V_j = 285$ ft/sec.

$\overline{q_j} = 96.5$ psf

3.2 General Take-Off Program

The take-off is considered to consist of a ground run in the air-cushion configuration, a transition, and a climb-out in the jet-flap configuration. It is more difficult to optimize the ground run and the transition with respect to distance than the climb-out, since an additional set of parameters enter into the optimisation problem, i.e., J_1/J_2 and θ_1. In Refs. 8 and 9 a number of ground runs were analysed, in which one or more of the parameters α, h'/c, J_1/J_2, θ_1 and J/J_T were programmed during the ground run to produce maximum acceleration, and thus, a minimum ground run distance. It was found that the most complex program, which involved the simultaneous variation of J_1/J_2, J/J_T and θ_2, did not yield substantially higher accelerations than the simplest program, in which all parameters except h'/c were held fixed. In view of the difficulties inherent in a complicated ground run program, only the two simplest ones are presented here. During both of these take-offs the peripheral jet configuration remains fixed. Both leading and trailing edge jets have the same strength and direction, i.e., perpendicular to the plane of the wing. In the first case the amount of thrust supplied to the peripheral jet is held fixed, at $J/J_T = 0.5$, while the height above ground is allowed to increase with forward speed. In the second ground run program the height above ground is held fixed at $h'/c = 0.108$ by varying J/J_T.

3.3 Calculation of Transition Speed and Height

In attempting to find a transition forward speed and height the main problem is that the lifting effectiveness of the air cushion—the lift augmentation—decreases with height, while that of the jet flap—the lift coefficient—increases with height above ground. If transition from air cushion to jet flap is made at large heights to take advantage of the higher lift coefficients of the jet flap at these heights, most of the installed thrust has to be diverted into the peripheral jet to maintain a large height. As a result little thrust is available for forward propulsion giving rise to low accelerations and a long ground run. If, on the other hand, transition is attempted at low heights to make use of the high lift augmentation of the air-cushion configuration there, the transition speed has to be fairly high to compensate for the low lift coefficients of the jet flap at these low heights. The resulting climb-angle would also be small and therefore the climb over a 50-ft. obstacle would give rise to a long climb-out distance.

To find the optimum transition point between the two extreme cases described above, the flight envelopes, h'/c vs qS/J_T, for both flight regimes-air cushion and jet flap—were calculated using experimental data and plotted in Fig. 13. Curves I represent the height above ground that can be attained

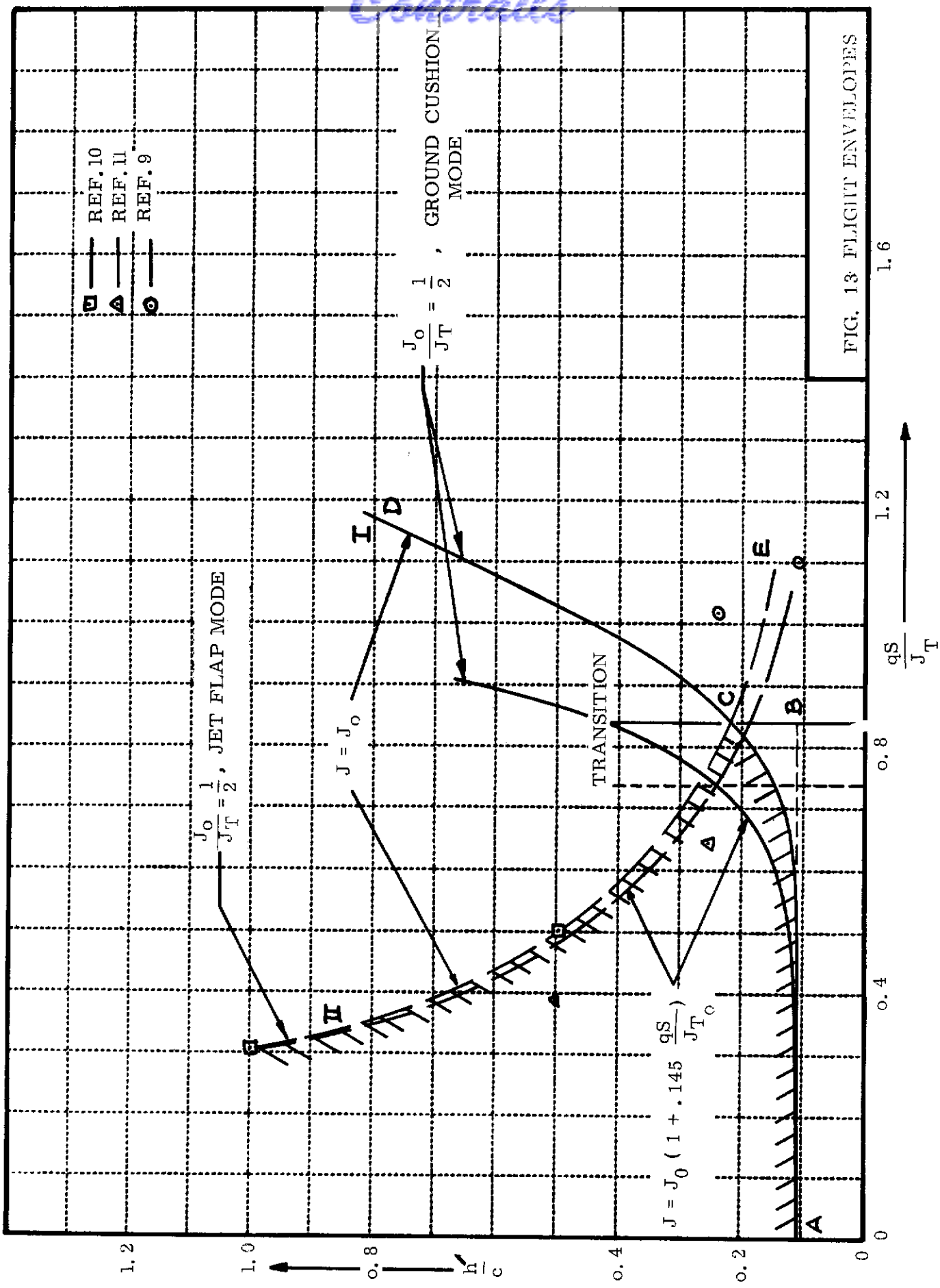

FIG. 13 FLIGHT ENVELOPES

by the vehicle in the air-cushion mode, if all of the thrust that can be made available is put into the peripheral jet. This corresponds to $J/J_T = 0.5$, which is the hovering value of J/J_T. Curves II represent the lowest forward speed at which the vehicle can fly in the jet-flap mode at a given height for the same maximum value of $J/J_T = 0.5$.

The two flight envelopes jointly define the region of (h'/c, qS/J_T) in which the vehicle can fly in either configuration (Region DCE); and point C gives the lowest possible transition speed, and the largest possible transition height at that speed.

Two sets of curves are shown on Fig. 13. The two labelled $J = J_o$ are based on the assumption that the cushion jet momentum flux remains constant as the forward speed of the vehicle increases. The other two curves are based on the assumption that the cushion air is supplied through a forward-facing intake, giving 100% ram recovery. Thus J increases with forward speed, viz.

$$J = J_o\left(1 + .145\,\frac{qS}{J_{T_o}}\right)$$

where subscript zero denotes the values at zero forward speed. The minimum transition speeds for the two cases are

$$\text{No ram recovery:} \quad \left(\frac{qS}{J_T}\right)_{\text{transition}} = 0.84$$

$$\text{100\% ram recovery:} \quad \left(\frac{qS}{J_T}\right)_{\text{transition}} = 0.73$$

The latter case is considered to be the more realistic one; however, it should be noted that the only effect of the ram recovery considered is the increase in allowable height at any speed resulting in the possibility of transition at lower speeds. The secondary effects of the pressure recovery on the characteristics of the engine, and the small variation of J_T along the take-off run were neglected for simplicity due to their dependence on the particular configuration.

Some scatter is evident in the data points for Curve II in Fig. 13. In particular, one of the data points from Ref. 9 does not follow the trend of those from Refs. 10 and 11. The reason for this is considered to be the existence of span-wise velocity components in the trailing edge jet. The jet

air at the center of the wing blows toward the wing tips at either side of the plane of symmetry of the wing. This causes a weak spot in the jet sheet which increases in extent as the height above ground increases. This results in a reduction of lift and an upward shift of Curve II in Fig. 13.

3.4 Calculation of Ground Run Distance

Program I: $J/J_T = 0.5$

In this program J/J_T is kept constant at its maximum value of 0.5 during the ground run while the height above ground is allowed to increase. The ensuing flight path corresponds to the segment AC of Curve I in Fig. 13. When the aircraft has entered the jet-flap regime at point C, transition is made to the jet-flap configuration and climb-out begins.

During the ground run the forward acceleration is given by

$$\frac{a}{g} = \frac{T_D}{W} - \frac{D}{W} - \frac{D_{mom}}{W} \tag{5}$$

$$= \frac{T_D}{W} - \frac{D}{J}\frac{J}{W} - \frac{D_{mom}}{J}\frac{J}{W} \; ; \tag{6}$$

since

$$\frac{T_D}{W} = \frac{J}{W} = \frac{1}{2}\frac{J_T}{W} = 0.35 \tag{7}$$

and

$$\frac{D_{mom}}{J} = \rho\frac{A_j \bar{V}_j . V}{J} \doteq \frac{V}{\bar{V}_j} = \sqrt{\frac{q}{\bar{q}_j}} \tag{8}$$

equation (6) becomes

$$\frac{a}{g} = 0.35 - 0.35\frac{D}{J} - 0.35\sqrt{\frac{q}{\bar{q}_j}}$$

$$= 0.35\left(1 - \frac{D}{J} - \sqrt{\frac{q}{\bar{q}_j}}\right) \tag{9}$$

It can be shown that the ground run distance R_1 as a function of qS/J_T is

$$\frac{R_1}{w} = \frac{1}{\rho g} \frac{J_T}{W} \int_0^{\frac{qS}{J_T}} \frac{1}{(a/g)} \, d\left(\frac{qS}{J_T}\right) \qquad (10)$$

Equation (10) can be integrated numerically. It is shown in Fig. 14 as a plot of R_1/w vs qS/J_T. R_1/w at transition can now be found by using the value of qS/J_T at point C in Fig. 13. The corresponding values of ground run distance and transition speed are, for $w = 20$ psf:

TABLE 2

GROUND RUN AND TAKE-OFF SPEEDS

	R_1 (ft)	V (m.p.h.)
No ram recovery	586	68
100% ram recovery	500	63

It was observed that the term D/J in Eq. (9) was not very large, and this suggested a simple analytical solution for R_1. By neglecting D entirely, Eq. (10) can be integrated for the case of no ram recovery to give

$$R_1 = -A \left[\ln (1 - B) + B\right] \qquad (10a)$$

where

$$A = 13.06 \, w \frac{J_D}{J} \frac{S}{A_j}$$

$$B = \frac{J}{J_D} \left(2 \frac{q_1 S}{J} \frac{A_j}{S}\right)^{1/2}$$

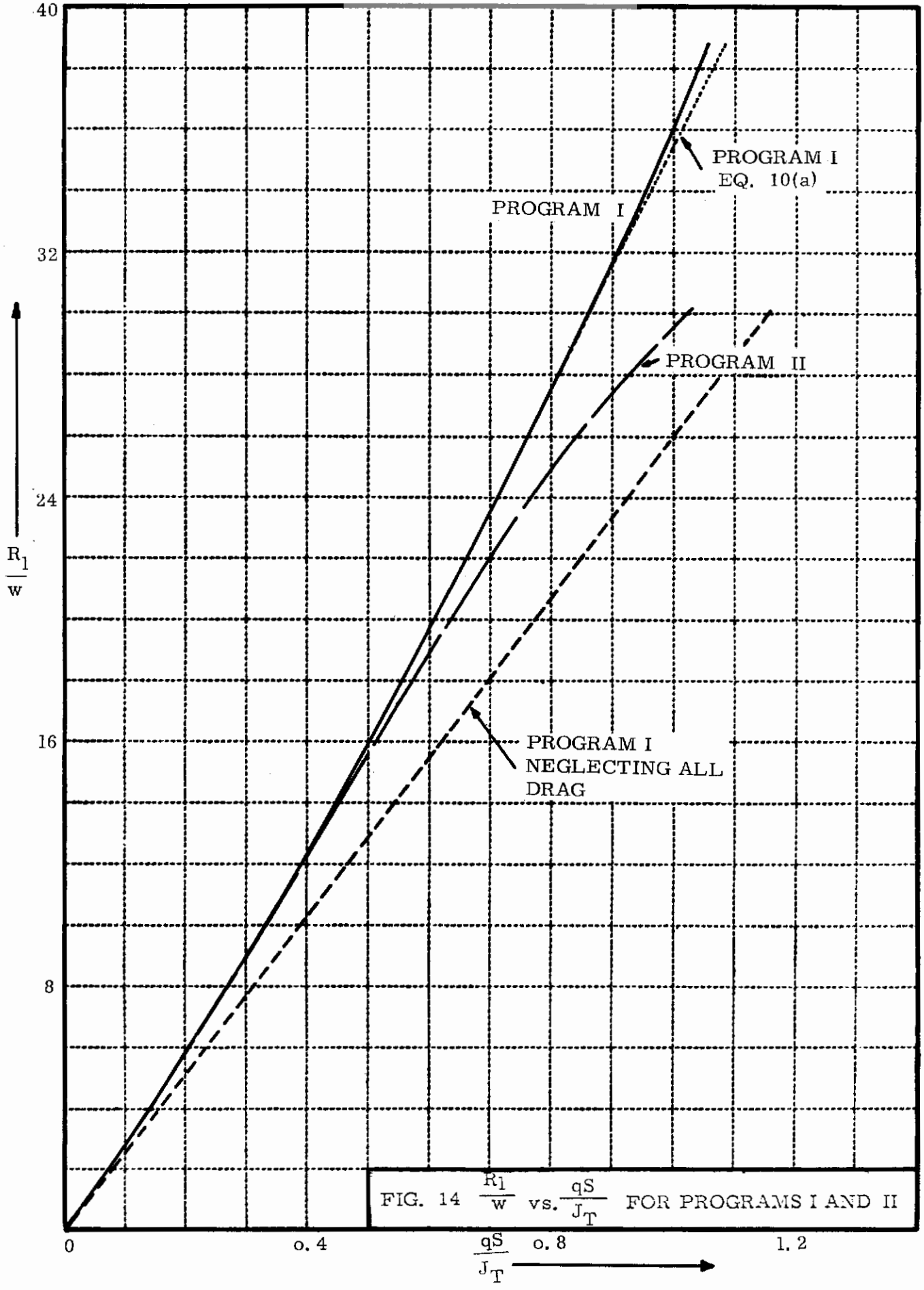

FIG. 14 $\frac{R_1}{w}$ vs. $\frac{qS}{J_T}$ FOR PROGRAMS I AND II

and

q_1 = value of q at transition speed

As shown on Fig. 14, Eq. (10a) gives correct results for Program 1 up to the transition speeds of interest. To show the importance of inlet momentum drag, the lowest curve on Fig. 14 is presented, for which both D and D_{mom} are taken to be zero.

Since Eq. (10a) is accurate for take-off Program 1, and since the latter is almost as good as the best program, the equation is useful for studying the effect of the main parameters. A chart of Eq. (10a) is presented on Fig. 15, showing the effect on R_1 of changing the propulsive thrust and the slot area ratio. Note from the equation that $R_1 \propto w$.

Program II, $h'/c = 0.108$

The ground run program for this case is represented by Curve ABC in Fig. 13. The height above ground is kept constant at $h'/c = 0.108$ as the aircraft accelerates from hovering to transition speed at point B. During acceleration the required J/J_T to keep the aircraft at constant height decreases. The excess J/J_T is diverted to forward propulsion in order to increase acceleration. At transition speed (point B) this excess J/J_T is diverted back into the peripheral jet, so that the height above ground increases while forward speed is kept constant, until the transition point C is reached. For this program

$$\frac{T_D}{W} = \frac{J_T}{W} - \frac{J}{W} \tag{11}$$

so that Eq. (6) becomes

$$\frac{a}{g} = \frac{J_T}{W} - \frac{J}{W}\left(1 + \frac{D}{J} + \frac{D_{mom}}{J}\right)$$

$$= 0.7 - \frac{1}{(L/J)}\left(1 + \frac{D}{J} + \sqrt{\frac{q}{\bar{q}_j}}\right) \tag{12}$$

for

$$\frac{J_T}{W} = 0.7,\ L = W,\ \frac{D_{mom}}{J} \doteq \sqrt{\frac{q}{\bar{q}_j}}$$

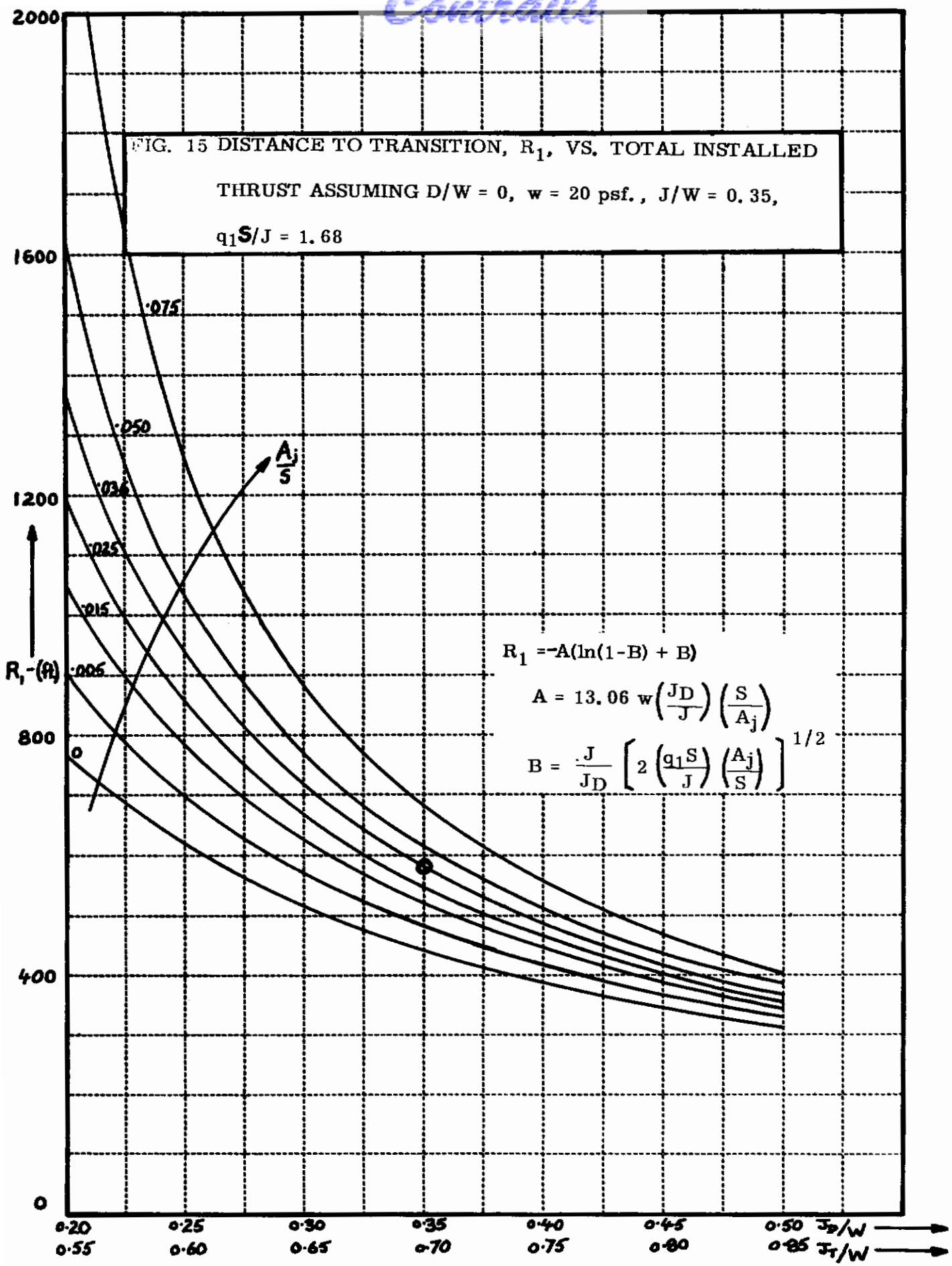

FIG. 15 DISTANCE TO TRANSITION, R_1, VS. TOTAL INSTALLED THRUST ASSUMING D/W = 0, w = 20 psf., J/W = 0.35, $q_1 S/J = 1.68$

Figure 14 shows R_1/w vs. qS/J_T for this program. The ground run distance corresponding to curve AB in Fig. 13 was found to be 510 ft. for w = 20 psf.

At point B, J/J_T is increased to 0.5 and the excess lift is used for flight-path curvature to go from B. to C. This rotation requires 68 ft. of horizontal distance. Therefore, the total ground run to point C for Case II is 578 ft., which is only 8 ft. less than in Case I. Thus, Program I is preferable to Program II, since the former is simpler.

3.5 Calculation of Climb-Out Distance

Climb-out takes place in the jet-flap mode at constant forward speed ($qS/J_T = 0.84$), $\alpha = 0$ and $\theta_2 = 35^o$ and consists of upwardly curved flight beginning at transition speed and height followed by a steady climb to a height of 50 ft. The aircraft is assumed to have a small angle of attack ($\alpha = 2^o$) just after transition to initiate rotation. However, during most of the rotation it is assumed that $\alpha = 0$, and $J/J_T = 0.5$, and that the necessary load factor is produced solely by the increase of C_L with height above ground. Under these conditions the maximum climb angle is $\gamma_{max} = 16.8^o$. When γ_{max} is reached, the load factor is reduced to 1 by reducing J/J_T and steady climb begins at $qS/J_T = 0.84$. Under these assumptions the distances covered during transition and steady climb to 50 ft. are $R_2 = 176$ ft. and $R_3 = 94$ ft. respectively for w = 20 psf. These values are conservative because (a) the flight path during transition could have been steepened by increasing α, (b) the maximum climb angle could have been increased to 29^o by diverting thrust from the jet flap to direct propulsion. A summary of the take-off distances is given in Table 3.

TABLE 3

TAKE-OFF DISTANCES FOR CASE I AND II

		R_1	R_2	R_3	TOTAL
Case I	No Ram	586	176	94	856
	100% Ram	500	211	72	783
Case II	No Ram	510+68	176	94	848

3.6 Control and Stability

Trim

In order to obtain conventional characteristics in cruise, it is assumed that the GETOL airplane has a normal tail. The wing-tail combination during take-off is analyzed as follows (see Fig. 16):

Equilibrium of moments requires that

$$L_w (x - x_w)c - L_t \; l_t = 0 \tag{13}$$

whence the C.G. position is given by

$$x = x_w + \frac{L_t}{L_W} \frac{l_t}{c} \tag{14}$$

The tail lift may be expressed in terms of the tail lift coefficient as

$$L_t = C_{L_t} \; qS_t$$

and we assume that the wing lift is approximately equal to the weight, $L_w \doteq W$, so that Eq. (14) becomes

$$x = x_w + \frac{C_{L_t} \; qS_t \; l_t}{Wc}$$

which is conveniently rearranged to give

$$x = x_w + V_H \left(\frac{J_T}{W}\right) C_{L_t} \left(\frac{qS}{J_T}\right) \tag{15}$$

This equation gives the allowable C.G. positions, from the standpoint of trim, for the wing-tail combination without any auxiliary control devices. Examples are plotted on Fig. 17 for the two take-off runs presented in Sec. 3.2; for $V_H = .5$, $J_T/W = .7$ and $C_{L_t} = \pm 1.0$, a value that is readily achieved. With these numerical data, the equation of the curves is

$$x = x_w \pm .35 \left(\frac{qS}{J_T}\right) \tag{15a}$$

Figure 17 shows that the tail provides a very significant trim capability, and that if the C.G. range is for example, .45 to .55 c, auxiliary

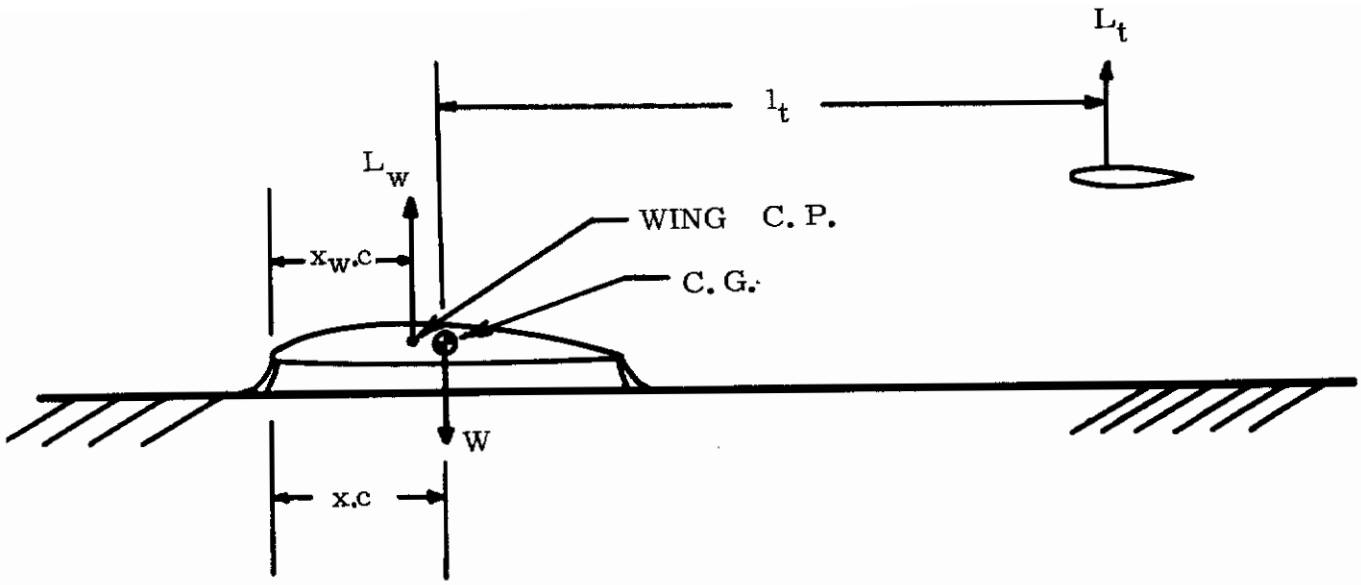

FIG. 16 WING AND TAIL FORCES DURING GROUND RUN

FIG. 17 TRIM CAPABILITY DURING TAKE-OFF(V_H=0.5)

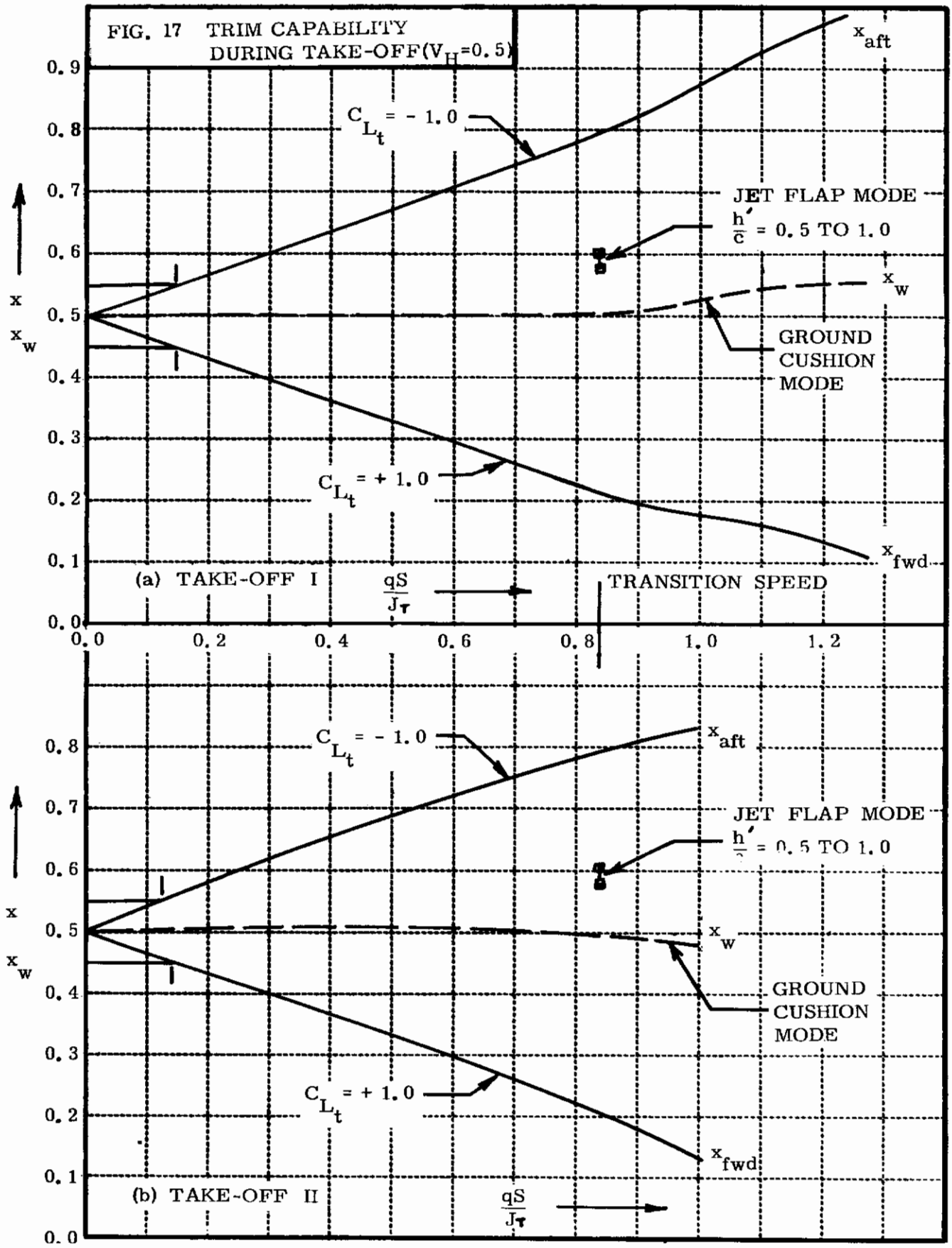

control is required only up to $qS/J_T = .15$, i.e. $V \doteq 30$ mph for the example cases.

The figure also shows the values of x_w for the wing in the jet flap mode for heights between 1/2 and one chord (from Ref. 10). It is evident that the trim change during transition from the ground cushion to the jet flap is not excessive, and is within the capability of the tail to balance.

Stability

From Fig. 16 the moment about the C.G. is

$$M = M_w - L_t l_t$$

whence it readily follows that

$$\frac{\partial}{\partial \alpha}\left(\frac{M}{Wc}\right) = \frac{\partial}{\partial \alpha}\left(\frac{M_w}{Wc}\right) - a_t V_H \left(\frac{J_T}{W}\right).\left(\frac{qS}{J_T}\right) \qquad (16)$$

Since the wing c.p. is very close to the mid chord during take-off at $\alpha = 0$, and the moments were measured about this point, we find it convenient to express the wing moment as

$$M_w = (M_w)_{c/2} + L_w (x - .5)\, c$$

whence

$$\frac{\partial}{\partial \alpha}\left(\frac{M_w}{Wc}\right) = \frac{\partial}{\partial \alpha}\frac{(M_w)_{c/2}}{Wc} + \frac{\partial}{\partial \alpha}\left(\frac{L_w}{W}\right)(x - .5) \qquad (17)$$

and

$$\frac{\partial}{\partial \alpha}\left(\frac{M}{Wc}\right) = \frac{\partial}{\partial \alpha}\frac{(M_w)_{c/2}}{Wc} + \frac{\partial}{\partial \alpha}\left(\frac{L_w}{W}\right)(x - .5) - a_t V_H \frac{J_T}{W}\left(\frac{qS}{J_T}\right) \qquad (18)$$

The criterion for static stability is that the RHS of Eq. (18) < 0. An estimate of the second term has been made--it varies from zero at zero forward speed to a maximum at take-off of the order of .03 (x - .5). For C.G. positions as far aft as x = .55, this term is then less than .0015, which can be neglected compared to the other terms. The approximate form of (18) (exact for x = .5) is then

$$\frac{\partial}{\partial \alpha}\left(\frac{M}{Wc}\right) = \frac{\partial}{\partial \alpha}\left(\frac{M_{wc/2}}{Wc}\right) - a_t V_H \frac{J_T}{W}\left(\frac{qS}{J_T}\right) \qquad (19)$$

For the same cases as treated above, and assuming $a_t = .07$ per deg., we get

$$\frac{\partial}{\partial \alpha}\left(\frac{M}{Wc}\right) = \frac{\partial}{\partial \alpha}\left(\frac{M_{wc/2}}{Wc}\right) - .0245\left(\frac{qS}{J_T}\right) \qquad (20)$$

Figure 18 shows the graphs of Eq. (20) for both take-off programs. It is seen that the wing alone is unstable at all speeds, but that adding the tail produces inherent stability before take-off speed is reached, i.e., above about V = 58 mph. For the lower range of speeds near hovering an auxiliary stabilization system is required. To provide a margin of stability in hovering, the stabilizer must be capable of supplying a synthetic pitch 'stiffness' of the order of

$$\frac{\partial}{\partial \alpha}\left(\frac{M}{Wc}\right) = -.015 \text{ per degree}$$

If this is produced by a vertical force located $2\frac{1}{2}$ chord lengths from the C.G., then the maximum force required at $\alpha = 5^o$ is

$$F = .03W$$

i.e. the stabilizing force required is about 3% of W. This represents an appreciable penalty, and indicates that research aimed at finding a configuration inherently stable at zero speed would be worth while.

When in the jet-flap mode, the data of Ref. 10 shows that at all heights above ground, the wing-alone neutral point is very close to the quarter-chord. It therefore follows that

$$\frac{\partial}{\partial \alpha}\left(\frac{M}{Wc}\right)_{\text{jet flap}} = \frac{C_{M_\alpha}}{C_L} = \frac{C_{L_\alpha}}{C_L}(x - .25)$$

With the C.G. at mid-chord (x = .5), and

$$C_L = \frac{W}{qS} = \frac{J_T}{qS} \cdot \frac{W}{J_T} = \frac{1}{.7}\frac{J_T}{qS}$$

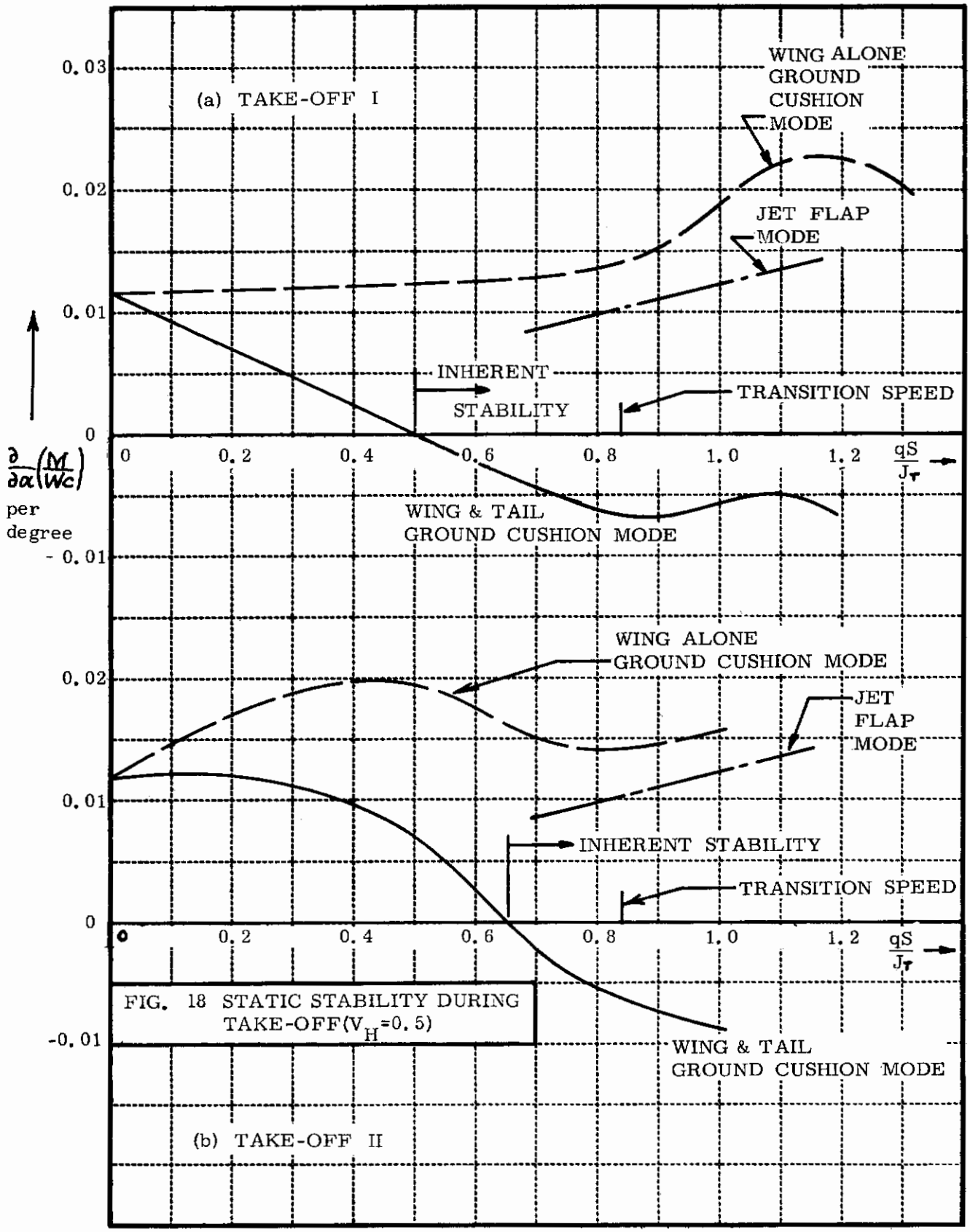

FIG. 18 STATIC STABILITY DURING TAKE-OFF(V_H=0.5)

we get

$$\frac{\partial}{\partial \alpha}\left(\frac{M}{Wc}\right)_{\text{jet flap}} = .175\, C_{L_\alpha}\left(\frac{qS}{J_T}\right)$$

The value of C_{L_α} at $\alpha = 0$, $C_\mu = .65$ and $h/c = 1.0$ from Ref. 10 is $C_{L_\alpha} = .070/^{\circ}$, which is taken as a representative value. Then we get

$$\frac{\partial}{\partial \alpha}\left(\frac{M}{Wc}\right)_{\text{jet flap}} = .0122\left(\frac{qS}{J_T}\right)$$

These values are also plotted on Fig. 18 and show that the change in static stability at transition is unimportant.

Neutral Point in Cruise

The stick-fixed neutral point of the cruise configuration, with the tail characteristics assumed, is estimated to be about

$$x_n = 0.65$$

without allowing for the usual adverse effect of a body. Even when the latter is included, it seems feasible to cater for C.G. positions around 50% chord, as required to keep the hovering trim moments small. If necessary, of course, a considerably larger tail volume ratio than 0.50 could be used. Thus we find that the C.G. locations required for hover, take-off, and cruise are all compatible.

Section 4

APPLICATION TO LANDING

4.1 Introduction

The requirements for landing are two-fold. Firstly, the required distance to stop after approaching over a 50-ft. obstacle must be not more than the take-off distance; and secondly, the vehicle must be capable of absorbing the energy associated with the remaining vertical velocity component after round-out. These two problem areas are dealt with below.

4.2 Landing Distance

The ground run part of the landing distance may be treated similarly to the ground run during take-off. Only one case is considered, in which $J/W = 0.35$ and remains constant, so that the height-speed curve is identical to that shown in Fig. 13. Assuming a 50% thrust reversability of the main engine (which is quite conservative), the deceleration at any point is given by

$$-\frac{a}{g} = 0.5 \times 0.35 + \frac{D_{mom}}{W} + \frac{D}{W}$$

where now the main thrust unit also contributes to the momentum drag, i.e.

$$\frac{D_{mom}}{W} = \frac{J_T}{W}\sqrt{\frac{q}{\bar{q}_j}}$$

Thus, the stopping distance R_4 as a function of speed is given in Fig. 19. Assuming that the same flight path is followed from 50 ft. to transition as in the take-off, then a comparison of Fig. 19 with Fig. 14 shows that the landing program is shorter than the take-off for any transition speed. In particular, for the higher transition speed used for take-off, $qS/J_T = 0.84$, the difference is 76 ft. Larger approach angles are possible and could be used to steepen the glide path still further, and lower wing loading at landing would also result in reduction of required distance. Thus, it is concluded that landing can always be made in a shorter distance than take-off.

4.3 Energy Absorption

In order to destroy the remnant of vertical velocity remaining after round-out, the normal shock absorbing qualities of landing gears must be

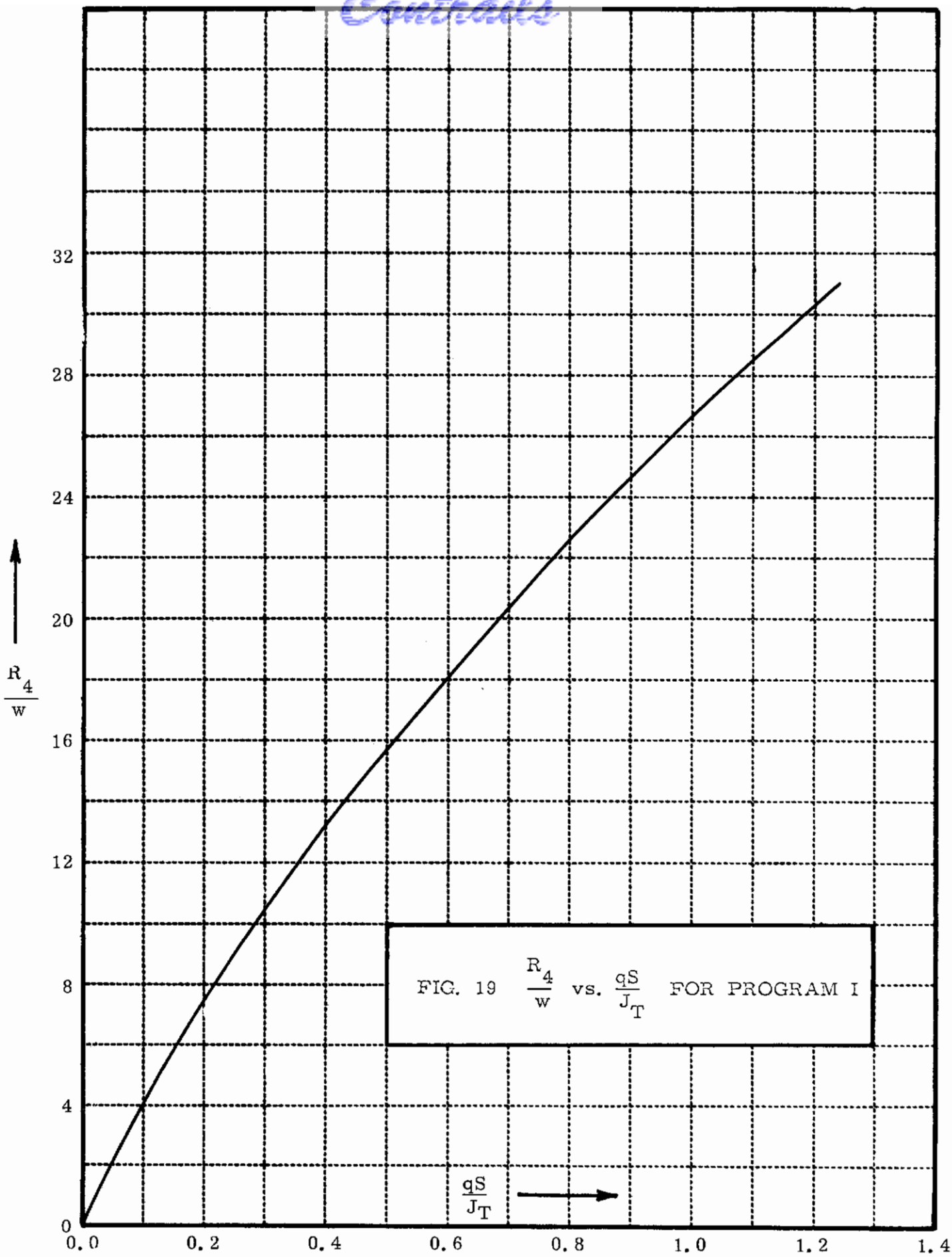

FIG. 19 $\frac{R_4}{w}$ vs. $\frac{qS}{J_T}$ FOR PROGRAM I

replaced by the aerodynamic properties of the cushion below the aircraft. This can absorb the vertical energy of the aircraft because of the increase of lift augmentation with decreasing height. Figure 20 shows L/J vs h'/c for various qS/J_T values around the transition speed. If the vehicle has a vertical velocity V_Z, the cushion must absorb energy of value $\frac{1}{2}mV_Z^2$, which can be considered as equivalent to the energy obtained from dropping the machine from a height H, i.e.,

$$mgH = \tfrac{1}{2}mV_Z^2 \qquad (21)$$

$$V_Z = \sqrt{2gH}$$

The cushion acts as an energy absorber for heights below that at which L = W at a given speed, i.e., for J/W = 0.35, L/J > 2.86 for energy absorption. Also, the lower limit of the vertical travel of the machine must be above h'/c = 0.108.

Thus, the drop height may be found at any fixed speed as

$$mgH = \int_{.108}^{b} (L - W)\, dh', \text{ where } b = h'/c \text{ for } L = W$$

or

$$\frac{H}{c} = \frac{J}{W} \int_{.108}^{b} \frac{L - W}{J}\, d\left(\frac{h'}{c}\right) = \frac{V_Z^2}{2gc}$$

H and V_Z are calculated and plotted as functions of qS/J_T in Fig. 21. Since the value of qS/J_T at transition was assumed to be 0.84, the corresponding allowable sinking speed is V_Z = 2.8 ft/sec. Figure 21 also shows, however, that the allowable sinking speed can be increased considerably by a small increase in transition speed. In fact, if the transition speed is increased to V = 79 mph, so that the ground run at landing becomes as long as the ground run at take-off, the corresponding allowable sinking speed becomes V_Z = 8.6 ft/sec. The associated flight path angle is 6°. These numerical values are again considered to be conservative since (i) a thrust reversal capability of only 0.5 was assumed--a larger value would allow a higher qS/J_T for the same landing distance, with a corresponding increase in the allowable V_Z;

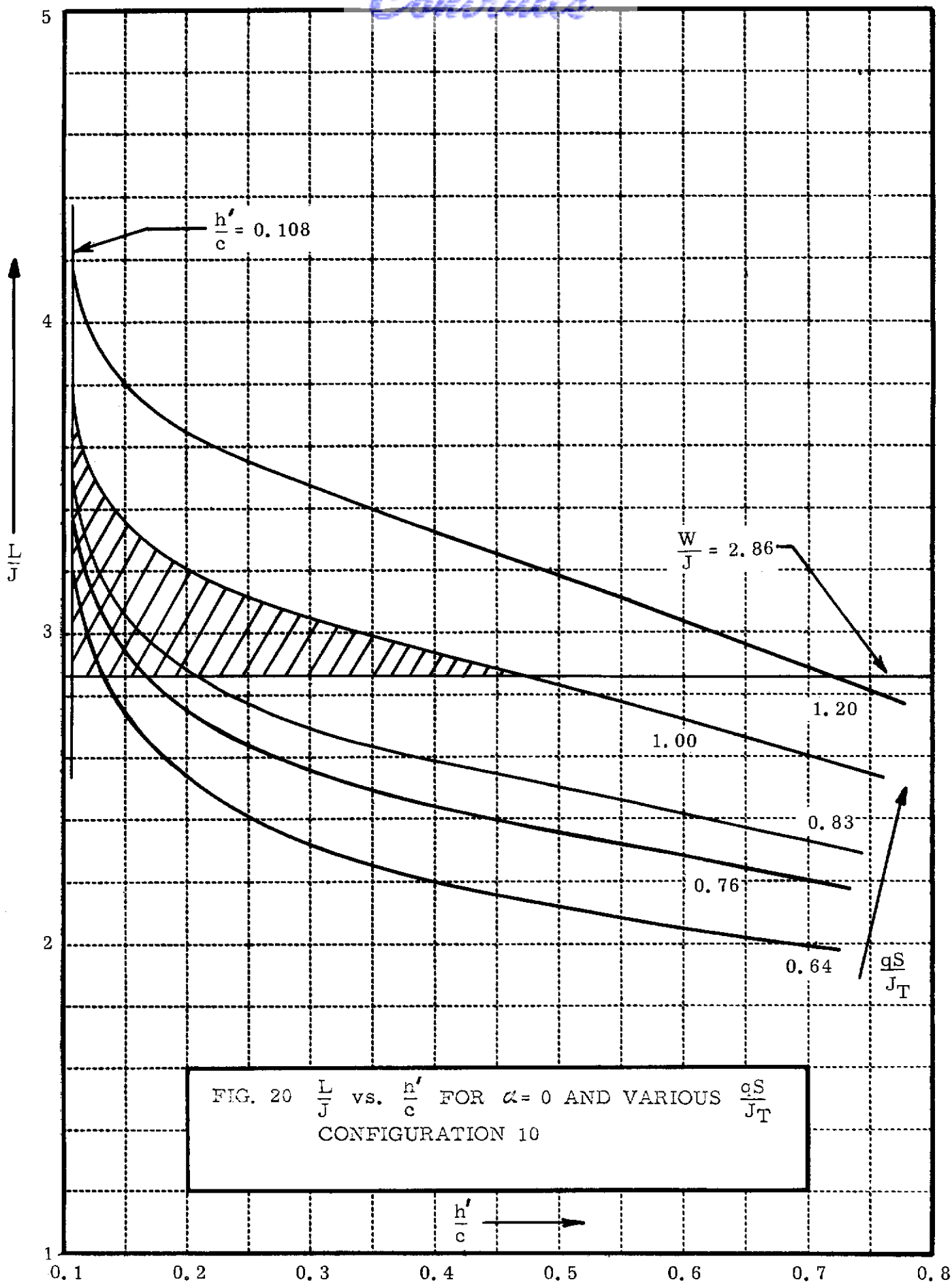

FIG. 20 $\frac{L}{J}$ vs. $\frac{h'}{c}$ FOR $\alpha = 0$ AND VARIOUS $\frac{qS}{J_T}$
CONFIGURATION 10

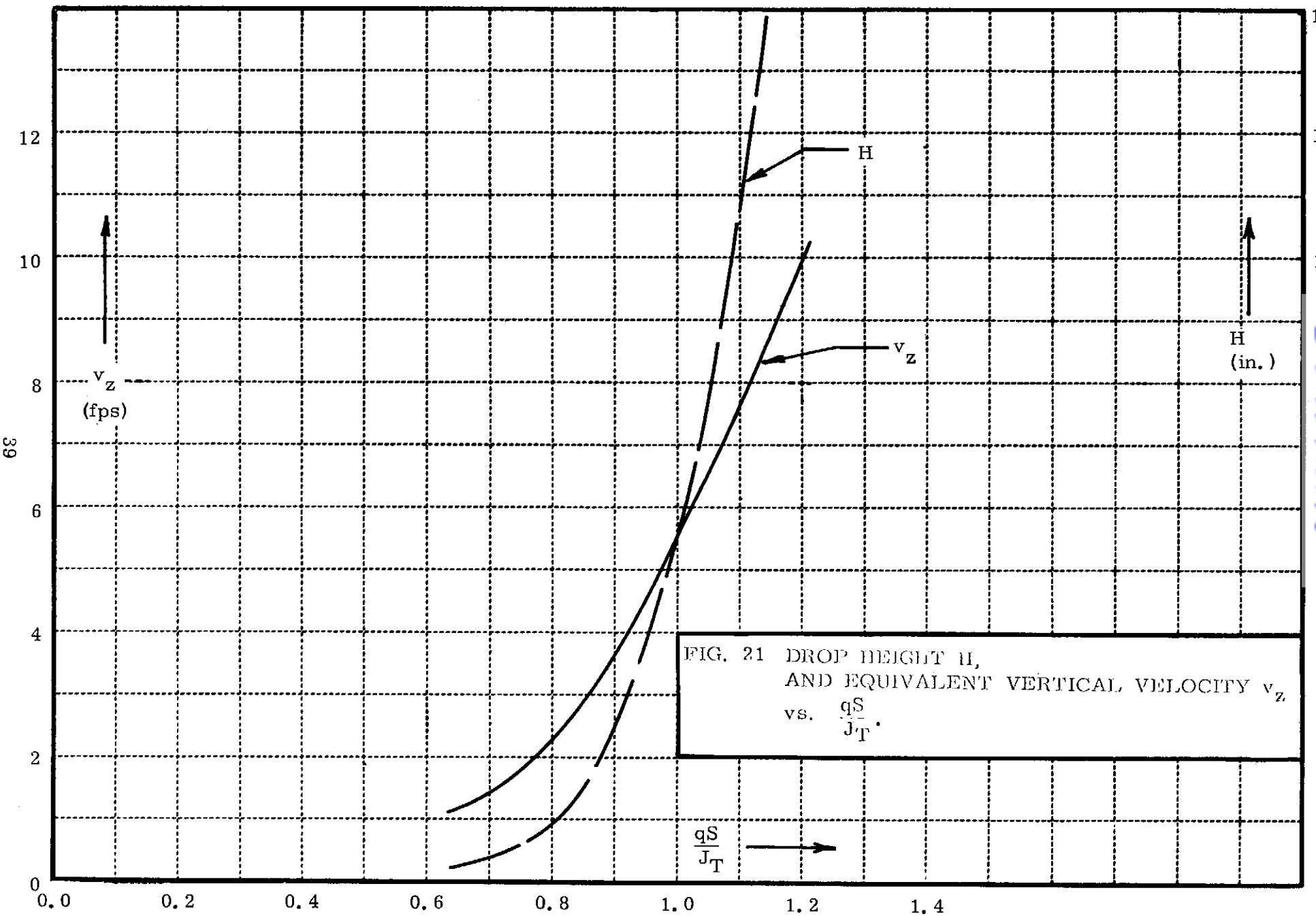

FIG. 21 DROP HEIGHT H, AND EQUIVALENT VERTICAL VELOCITY v_z vs. $\frac{qS}{J_T}$.

(ii) the poor momentum flux distribution in the jet curtain is thought to give rise to low values of L/J; and (iii) reducing the minimum height below $h'/c = 0.108$ would allow higher values of V_z.

It is appropriate here to consider the behaviour of the vehicle after it has reached zero sinking speed. Since at this point $L > W$, the vehicle tends to rise again, and the ensuing flight path would be oscillatory. Tests conducted on the UTIAS circular track* show, however, that these oscillations are highly damped.

---

* See Figure G. 2. 2, UTIAS Annual Progress Report, 1963.

Section 5

CONCLUSIONS

Realistic data, thought to be conservative, have been presented on the performance and stability aerodynamics of a GETOL wing. They show that a capability exists for achieving short field performance, i.e., less than 800 ft. to clear 50 ft., with a minimum ground clearance of 10% chord. For a 20,000 lb. airplane with wing loading of 20 psf, the clearance is about 1.6 ft. The total thrust required, lifting plus propulsive, is about 70% of the weight. The wing tested has an aspect ratio of 4, and hence would be best suited, from the cruise standpoint, to a short-to-medium range subsonic airplane.

The trim and stability problems are not prohibitive. Although the wing alone is unstable in pitch, the addition of a conventional tail produces inherent stability before take-off speed is reached and provides adequate trim capability.

Trim and stability in hovering can be achieved by 'brute force'—by the application of a controllable vertically-downward thrust at the tail of the order of 5% W. However, an inherent aerodynamic solution based on the cushion properties should be sought. The requirements on C.G. position for take-off and normal flight are compatible, requiring a tail volume ratio of about 0.5 or greater.

The practicability and utility of such a vehicle can only be properly assessed by a fairly detailed design and operational study. It is suggested that such a study would be a worthwhile project for the aircraft industry.

Section 6

REFERENCES

1. Von Glahn, U. "Exploratory Study of Ground Proximity Effects on Thrust of Annular and Circular Nozzles." NACA TN. 3982, April 1957.

2. Frost, J.C.M. "The Canadian Contribution to the Ground Cushion Story." Can. Aero. Journ. 7, 8, Oct. 1961.

3. Stepniewski, W.Z. "Performance Possibilities of Subsonic Airplanes Taking-Off and Landing on the Ground Cushion." Proceedings, Symposium on Ground Effect Phenomena, Princeton University, Oct. 1959.

4. Vertol Division The Boeing Co. "Research Program to Determine the Feasibility and Potential of the Ground Effect Take-Off and Landing (GETOL) Configuration." U.S. Army, TRECOM, TCREC Tech. Rept. 62-63, Dec. 1962.

5. Reeder, Walter D. & McDonald, R.W. "GETOL Aircraft: A Research Status Report." IAS Paper No. 62-182, June 1962.

6. Alexander, A.J. "Experiments on a 70° Cropped Delta Wing with 90° Downward Deflected Peripheral Blowing." College of Aeronautics, Cranfield, CoA note 131, Sept. 1962.

7. Dau, K. "Characteristics of a Rectangular Wing With a Peripheral Jet in Ground Effect, Part I." UTIA Tech. Note 56, Sept. 1961.

8. Davis, J.M. "Characteristics of a Rectangular Wing With a Peripheral Jet in Ground Effect, Part II." UTIA Tech. Note 59, May 1962.

9. Surry, D. "Characteristics of a Rectangular Wing with a Peripheral Jet in Ground Effect, Part III." UTIA Tech. Note 77, Sept. 1964.

10. Vogler, R. D. and Turner, T. R. "Wind-Tunnel Investigations at Low Speeds to Determine Flow Field Characteristics and Ground Influence on a Model with Jet-Augmented Flaps." NACA TN 4116, Sept. 1957.

11. Korbacher, G. K. & Sridhar, K. "A Review of the Jet Flap." UTIA Review No. 14, May, 1960.

Unclassified
Security Classification

DOCUMENT CONTROL DATA - R&D
(Security classification of title, body of abstract and indexing annotation must be entered when the overall report is classified)

1. ORIGINATING ACTIVITY (Corporate author) University of Toronto Institute of Aerospace Studies Toronto, Canada	2a. REPORT SECURITY CLASSIFICATION Unclassified 2b. GROUP N/A

3. REPORT TITLE
AERODYNAMICS OF A RECTANGULAR WING WITH A PERIPHERAL JET FOR AIR CUSHION TAKE-OFF AND LANDING

4. DESCRIPTIVE NOTES (Type of report and inclusive dates)
Technical Documentary Report - May 1959 to Sept 1964

5. AUTHOR(S) (Last name, first name, initial)
Dau, K.
Etkin, B.
Surry, D.

6. REPORT DATE	7a. TOTAL NO. OF PAGES	7b. NO. OF REFS
September 1965	54	11

8a. CONTRACT OR GRANT NO.	9a. ORIGINATOR'S REPORT NUMBER(S)
AF33(657)-8451 b. PROJECT NO. 8219 c. Task: 821907 d.	AFFDL TR 65-59 9b. OTHER REPORT NO(S) (Any other numbers that may be assigned this report) --

10. AVAILABILITY/LIMITATION NOTICES
None

11. SUPPLEMENTARY NOTES	12. SPONSORING MILITARY ACTIVITY
None	AFFDL (FDCC) Wright-Patterson AFB, Ohio 45433

13. ABSTRACT

Subsonic wind tunnel experiments on a GETOL wing are reported. The main results relevant to performance, stability and control are presented, and applied to a hypothetical vehicle. Short-field capability is demonstrated to be possible. Stability and control problems are analyzed, and shown not to be prohibitive.

DD FORM 1 JAN 64 1473

Unclassified
Security Classification

Unclassified
Security Classification

14. KEY WORDS	LINK A		LINK B		LINK C	
	ROLE	WT	ROLE	WT	ROLE	WT
STOL						
Ground Effects						
Stability & Control						
Aerodynamics						
Peripheral Jet						

INSTRUCTIONS

1. ORIGINATING ACTIVITY: Enter the name and address of the contractor, subcontractor, grantee, Department of Defense activity or other organization *(corporate author)* issuing the report.

2a. REPORT SECURITY CLASSIFICATION: Enter the overall security classification of the report. Indicate whether "Restricted Data" is included. Marking is to be in accordance with appropriate security regulations.

2b. GROUP: Automatic downgrading is specified in DoD Directive 5200.10 and Armed Forces Industrial Manual. Enter the group number. Also, when applicable, show that optional markings have been used for Group 3 and Group 4 as authorized.

3. REPORT TITLE: Enter the complete report title in all capital letters. Titles in all cases should be unclassified. If a meaningful title cannot be selected without classification, show title classification in all capitals in parenthesis immediately following the title.

4. DESCRIPTIVE NOTES: If appropriate, enter the type of report, e.g., interim, progress, summary, annual, or final. Give the inclusive dates when a specific reporting period is covered.

5. AUTHOR(S): Enter the name(s) of author(s) as shown on or in the report. Enter last name, first name, middle initial. If military, show rank and branch of service. The name of the principal author is an absolute minimum requirement.

6. REPORT DATE: Enter the date of the report as day, month, year; or month, year. If more than one date appears on the report, use date of publication.

7a. TOTAL NUMBER OF PAGES: The total page count should follow normal pagination procedures, i.e., enter the number of pages containing information.

7b. NUMBER OF REFERENCES: Enter the total number of references cited in the report.

8a. CONTRACT OR GRANT NUMBER: If appropriate, enter the applicable number of the contract or grant under which the report was written.

8b, 8c, & 8d. PROJECT NUMBER: Enter the appropriate military department identification, such as project number, subproject number, system numbers, task number, etc.

9a. ORIGINATOR'S REPORT NUMBER(S): Enter the official report number by which the document will be identified and controlled by the originating activity. This number must be unique to this report.

9b. OTHER REPORT NUMBER(S): If the report has been assigned any other report numbers *(either by the originator or by the sponsor)*, also enter this number(s).

10. AVAILABILITY/LIMITATION NOTICES: Enter any limitations on further dissemination of the report, other than those imposed by security classification, using standard statements such as:

(1) "Qualified requesters may obtain copies of this report from DDC."

(2) "Foreign announcement and dissemination of this report by DDC is not authorized."

(3) "U. S. Government agencies may obtain copies of this report directly from DDC. Other qualified DDC users shall request through _____."

(4) "U. S. military agencies may obtain copies of this report directly from DDC. Other qualified users shall request through _____."

(5) "All distribution of this report is controlled. Qualified DDC users shall request through _____."

If the report has been furnished to the Office of Technical Services, Department of Commerce, for sale to the public, indicate this fact and enter the price, if known.

11. SUPPLEMENTARY NOTES: Use for additional explanatory notes.

12. SPONSORING MILITARY ACTIVITY: Enter the name of the departmental project office or laboratory sponsoring *(paying for)* the research and development. Include address.

13. ABSTRACT: Enter an abstract giving a brief and factual summary of the document indicative of the report, even though it may also appear elsewhere in the body of the technical report. If additional space is required, a continuation sheet shall be attached.

It is highly desirable that the abstract of classified reports be unclassified. Each paragraph of the abstract shall end with an indication of the military security classification of the information in the paragraph, represented as *(TS), (S), (C), or (U)*.

There is no limitation on the length of the abstract. However, the suggested length is from 150 to 225 words.

14. KEY WORDS: Key words are technically meaningful terms or short phrases that characterize a report and may be used as index entries for cataloging the report. Key words must be selected so that no security classification is required. Identifiers, such as equipment model designation, trade name, military project code name, geographic location, may be used as key words but will be followed by an indication of technical context. The assignment of links, rules, and weights is optional.

Unclassified
Security Classification